RM E55F21

NACA RM E55F21

NACA

RESEARCH MEMORANDUM

EXPERIMENTAL STUDY OF SHOCK-POSITIONING METHOD OF RAM-JET-ENGINE CONTROL

By Herbert G. Hurrell, George Vasu, and
William R. Dunbar

Lewis Flight Propulsion Laboratory
Cleveland, Ohio

NATIONAL ADVISORY COMMITTEE
FOR AERONAUTICS

WASHINGTON

August 29, 1955
Declassified October 31, 1958

NATIONAL ADVISORY COMMITTEE FOR AERONAUTICS

RESEARCH MEMORANDUM

EXPERIMENTAL STUDY OF SHOCK-POSITIONING METHOD OF RAM-JET-ENGINE CONTROL

By Herbert G. Hurrell, George Vasu, and William R. Dunbar

SUMMARY

Ram-jet-engine control by shock positioning was investigated on a 16-inch fixed-geometry ram jet at free-stream Mach numbers from 1.50 to 1.98. The continuous-acting, closed-loop system with proportional-plus-integral control action was subjected to disturbances in fuel flow, Mach number, angle of attack, and exhaust area. Steady-state and dynamic performance is presented.

The control method appears to offer adequate control of ram-jet-engine operation. Response times less than 0.1 second (90-percent reduction of error) were obtained with a stable system. The minimum response time (0.05 sec) approached the limit imposed by the system dead time. By providing a margin of operation in steady state from the region of diffuser buzz, transients into this region could be made without incurring buzz.

INTRODUCTION

The ram-jet engine is well suited for the propulsion of supersonic guided missiles. For such application, the performance of the power plant must be closely controlled throughout the flight plan. Adequate engine controls, therefore, must be developed for the ram jet if its capabilities for missile propulsion are to be fully utilized.

Analyses have been made that indicate the control requirements and suggest methods for controlling the ram-jet engine, but the experimental work has been rather limited. The control of a ram-jet engine with a variable exhaust area is analyzed in reference 1. Control requirements of a fixed-geometry ram jet for long-range missile application are discussed in reference 2. The latter reference indicates that control of the ram-jet engine should be accomplished by controlling the operation of its diffuser. Various systems of this type are proposed in reference 2.

One method of controlling the operation of the ram-jet diffuser is called shock positioning. This designation is given to the control technique in which the diffuser operating point is controlled by using the sharp pressure change across the shock to provide a signal indicative of shock position.

In order to evaluate shock positioning as a method of ram-jet-engine control, a continuous-acting closed-loop control system for shock-wave positioning was experimentally investigated. The investigation was conducted at the NACA Lewis laboratory as part of a test program in which the dynamics of the ram jet and several diffuser control techniques were studied. The tests were performed on a 16-inch fixed-geometry ram-jet engine in the 8- by 6-foot supersonic wind tunnel. Preliminary results of the entire program are briefly reported in reference 3. The present report presents a more complete and detailed evaluation of the shock-positioning system.

The dynamic and steady-state performance of the shock-positioning system was investigated for three design positions of the shock. The three positions were selected to give the following types of diffuser operation in steady state: well supercritical, near critical, and slightly subcritical. For each design position, transient operating conditions were imposed by disturbances in fuel flow, Mach number, angle of attack, and engine exhaust area. The following range of simulated flight conditions was covered: Mach numbers from 1.50 to 1.98, pressure altitudes from 26,500 to 36,500 feet, and angles of attack from zero to 10°.

CONTROL PRINCIPLES

Engine Considerations

The propulsive thrust of a fixed-geometry ram-jet engine at any flight condition is determined by the total-temperature ratio achieved in the burner. This temperature ratio also determines the operating point of the ram-jet diffuser. Positive control of the ram-jet engine, therefore, can be assured by the control of diffuser operation.

Diffuser operation is directly related to the position of the normal shock wave. The control of shock position, therefore, will control the operation of the diffuser and, hence, of the engine.

The relation between diffuser operating point and shock position is determined by the internal area variation of the diffuser. Diffuser operation with the shock at the minimum area is termed critical. Maximum, or near maximum, diffuser pressure ratio (diffuser-exit total pressure to free-stream static pressure) is obtained with the shock at

its critical position. If the engine temperature ratio is increased beyond that required for critical operation, the shock moves ahead of the inlet (lip); such operation is called subcritical. Subcritical operation is usually accompanied by a flow instability called diffuser buzz. Because of the violently pulsing pressures throughout the engine during buzz, subcritical operation is generally undesirable. As the temperature ratio is decreased from that required for critical operation, the shock moves downstream of the minimum area; such operation is termed supercritical. The diffuser pressure ratio for supercritical operation decreases as the shock occurs at larger areas and, hence, becomes more intense.

The desired diffuser operating point for a particular ram jet, of course, is dependent upon the mission for which the missile is designed. For long-range missiles, it is normally desirable to operate the diffuser at its most efficient point, that is, critical or near critical. A margin of operation from the subcritical region, however, may be necessary in order to avoid buzz during transient operation imposed by disturbances (such as gusts and changes in angle of attack) during flight. A supercritical operating point, therefore, is often required.

Shock-Positioning Technique

The way the shock can be positioned to give a specified diffuser operating point is illustrated in figure 1. The upper portion of this figure shows the relation of diffuser-exit total pressure to engine total-temperature ratio for a typical fixed-geometry ram jet at a given flight condition. The lower portion of the figure shows the variation with temperature ratio of the static pressure sensed by a control tap slightly downstream of the diffuser minimum area. The abrupt increase in this pressure with increasing temperature ratio is caused by the passage of the shock past the pressure tap. Assume, for example, that in order to provide a margin from the subcritical region it is necessary to operate the diffuser supercritically and with a value of exit total pressure designated by A in figure 1. At this diffuser operating point, the shock will be approximately at the control tap, and the static pressure sensed by this tap will have the value indicated as B in the figure. Controlling this static pressure at the value B, therefore, will hold the shock at the position required for the specified diffuser operation.

With the fixed-geometry ram jet, of course, the control of the static pressure considered in figure 1 must be accomplished by manipulation of the engine fuel flow. If the fuel flow is too low, the shock will be downstream of the control tap; the controlled pressure will then be less than the reference setting (B), and the control should increase fuel flow. For high fuel flow, the shock will be ahead of the control tap, resulting in a pressure greater than the reference. The control should, therefore,

decrease fuel flow. When the fuel flow is correct for the reference setting, the shock will be approximately at the tap location; the diffuser will then be at the specified operating point.

Control System Investigated

As noted previously, the shock position required for a given application of the ram jet may vary both with the flight plan and the necessary margin from the subcritical region of operation. In order to study the control problems associated with positioning the shock at different diffuser locations, the control system was investigated for three design locations of the shock. The design locations were selected to illustrate extremes in regard to providing steady-state operating margins from the buzz region. The locations selected are shown in figure 2 on a sketch of the forward portion of the ram-jet diffuser. This figure also shows the axial variation of the flow passage area. Two shock locations were chosen to give supercritical operation. The first, 15 inches downstream of the diffuser inlet, was at an area considerably greater than the minimum area and provided a rather large margin of operation from the buzz region. The second, 6 inches downstream of the diffuser inlet, was at an area just slightly greater than the minimum area and provided only a small margin. Since the engine used could be operated slightly subcritically with no appreciable buzz, a shock position corresponding to slight subcritical operation was chosen for the third design location of the shock. This third location was at the diffuser inlet, as shown in figure 2, and gives no practical margin from the buzz region.

The control system positioned the shock to the three design locations by the control of differential static pressures. Differential pressures were used in an effort to compensate for variable flight conditions. The static pressures at the design locations of the shock were subtracted from diffuser static pressures further upstream by differential pressure sensors. The location of the pressure taps is shown in figure 2. (Symbols are defined in appendix A.) The controlled pressure differences were called Δp_I, Δp_{II}, and Δp_{III} for the design shock locations at the 15-inch station, 6-inch station, and inlet, respectively. The control system was designated Δp_I control, Δp_{II} control, or Δp_{III} control according to the variable controlled.

The steady-state variation of the controlled variables (Δp_I, Δp_{II}, and Δp_{III}) with the manipulated variable (fuel flow) is shown in figure 3. The relation between the controlled variables and fuel flow was determined for three Mach numbers and the specific ambient static pressures that existed in the tunnel test section at these Mach numbers. The angle of attack was zero. At low fuel flows the shock is near the diffuser exit, and supersonic flow exists at the control pressure taps. The

controlled variables are constant for this condition. As fuel flow is increased, the shock moves upstream. Each controlled variable increases rapidly with fuel flow as the shock passes its downstream pressure tap. As seen in figure 3(a), Δp_I decreases again at a fast rate as the shock passes its upstream tap which is located at the diffuser inlet. The shock does not reach the upstream tap location for Δp_{II} (fig. 3(b)) and Δp_{III} (fig. 3(c)) at the fuel flows involved.

The reference settings (desired values of the controlled variables) are also shown in figure 3. A constant reference setting was used throughout the Mach number range with Δp_I control (fig. 3(a)). This reference setting was selected to give a shock position close to the design location (15-in. station) at a Mach number of 1.98 and zero angle of attack. With the use of a constant reference, however, somewhat different shock positions are to be expected at the other simulated flight conditions, especially at a Mach number of 1.50. This Mach number is appreciably below the design Mach number (1.89) of the ram jet, and vastly different flow conditions exist in the diffuser than at Mach numbers nearer the design value. Figure 3(a) indicates the shock will be positioned considerably upstream of the design location at a Mach number of 1.50. This is evident since the portion of the Δp_I curve for a Mach number of 1.50 between its minimum and peak values represents shock travel from approximately the 15-inch station to the 2-inch station (minimum area).

Constant reference settings were also used with Δp_{II} control (fig. 3(b)) and Δp_{III} control (fig. 3(c)) for Mach numbers of 1.98 and 1.79. Reset references, however, were provided for these controls at a Mach number of 1.50 in order to maintain a nearly constant shock position over the range of Mach numbers.

The block diagram of the control system is shown in figure 4. The feedback path consisted of a variable-reluctance sensor in combination with a carrier amplifier. The reference setting was made by adjusting the input bridge circuit of the carrier amplifier such that the amplifier output would be zero for the desired value of Δp. The carrier amplifier, therefore, also served as the error detecting device; its output V_1 was the error signal. A value of Δp greater than the reference setting resulted in positive V_1. The necessary reversal of sign for negative feedback was accomplished in the controller. A positive V_1 gave a negative controller output V_2, which resulted in a fuel flow decrease. The controller provided proportional-plus-integral control action. Frequency-response data for the engine had indicated this type of control was desirable. The coefficient K of the controller function and the integrator time constant τ were variable, as shown in the controller wiring diagram in figure 5.

APPARATUS

Ram-Jet Engine

The engine used in the investigation was a 16-inch-diameter ram jet and is shown in figure 6. The engine and its performance are discussed in detail in reference 4. The shock wave generated by the 25° (half-angle) conical spike intersected the inlet lip of the convergent-divergent diffuser at a Mach number of 1.89. The combustion chamber contained a can-type burner which was partially shrouded. The six spray nozzles of the primary fuel system were located within the shroud, and the secondary fuel was sprayed outside the shroud from 16 nozzles mounted in a circular manifold. In addition, a constant pilot fuel flow of 50 pounds per hour was used throughout the test program. The exit area of the conical convergent exhaust nozzle was equal to 0.69 of the combustion-chamber area.

Test Facilities

The installation of the ram-jet engine in the 8- by 6-foot supersonic tunnel is shown in figure 7. The exit plug was used to impose transients on the controlled engine by rapid changes in exhaust area. The exhaust area of the engine could be reduced from 0.69 to 0.54 of the combustion-chamber area by full forward movement of the plug. The maximum change required about 0.1 second. Pivoting the support strut with the inlet plate installed on the engine gave transients in Mach number. A photograph of this plate mounted on the engine is shown in figure 8. When the engine-plate combination was inclined to the tunnel flow direction, the flow expansion at the leading edge of the plate produced Mach numbers higher than the concurrent tunnel Mach number. This technique is discussed in reference 5. The plate was designed for transients within a Mach number range of 1.70 to 1.90. The full transient was made in about 0.75 second. When disturbances in angle of attack were made, the inlet plate was not installed. Pivoting the support strut produced transients in angle of attack from zero to 10° in approximately 1.0 second.

Control Fuel System

The control operated the secondary fuel system only. The primary fuel flow was held constant at a value giving satisfactory combustion. The fuel used was MIL-F-5624B, amendment 1, grade JP-4.

The secondary fuel system was designed for fast response and stability. A diagram of this system is presented in figure 9. The system consisted of an electrohydraulic servo system and a specially designed fuel valve. The closed-loop servo system provided a linear relation between the input voltage V_2 and the position of the throttle in the

fuel metering valve. The fuel valve incorporated a fast-acting relief valve which maintained a constant pressure differential across the throttle; thus fuel flow was a function of throttle position only. A fuel system of this type is discussed in detail in reference 6.

The dynamic performance of the fuel system as installed for the investigation is presented in figure 10. The figure shows the frequency-response characteristics of fuel-nozzle pressure drop to servo input voltage. The performance includes the dynamic effects of the piping required for the installation. Because the fuel system had to be located above the tunnel, rather long piping as well as a short length of flexible hose was required.

Controller and Instrumentation

An electronic differential analyzer was used as the controller. The proportional-plus-integral control action was provided by the use of high-gain direct-current operational amplifiers and associated plug-in input and feedback impedances. Fuel-flow disturbances to the control system were made by the addition of step changes to the output voltage of the controller.

A description of the instrumentation used in the control system and in the recording of the data is presented in appendix B. The response of the transient instrumentation is also given in appendix B. Carrier amplifiers were used with the transducers, and the amplifier output signals were recorded by a galvanometric oscillograph and a direct-inking 6-channel recorder. Signals from the controlled variables were fed to the controller, as well as to the recorders.

The controller, carrier amplifiers, and recorders were installed in the tunnel control room. The equipment is shown in figure 11. The equipment not designated in the figure was used in the investigation of the engine dynamics.

TEST PROCEDURE

The steady-state and dynamic performance of the controlled engine was investigated over a range of simulated flight conditions. The Mach number range was 1.50 to 1.98. The angles of attack investigated were zero and 10°. A change in the free-stream Mach number of the tunnel produced a change in the ambient static pressure. The relation of this pressure p_0 to the Mach number M_0 is shown in the following table. The free-stream total temperature T_0 of the tunnel is also given.

M_0	p_0, lb/sq ft abs	T_0, °R
1.50	730	565
1.79	545	585
1.98	460	610

The steady-state performance of the controlled engine was obtained by putting the control system in operation and then recording pertinent data at the various simulated flight conditions. Both the steady-state and transient instrumentation were used.

To provide stability information, recordings from the transient instrumentation were made at various controller settings with the engine in steady state.

Transient response was determined by subjecting the closed-loop system to positive and negative steps in controller output (fuel servo input) voltage. Fuel-flow disturbances of various magnitudes were produced by these steps. The range of disturbance magnitudes (278 to 1390 lb/hr) was about 8 to 48 percent of the fuel flow for critical operation of the engine. The disturbances were made for various settings of the controller gain and integrator time constant.

Additional transient operation was imposed by disturbances in Mach number, angle of attack, and exhaust area. A transient in free-stream static pressure also occurred with the Mach number disturbance produced by the inclined-plate technique.

Data for calibration of the oscillograms and the direct-inked recordings were taken with the steady-state instrumentation.

RESULTS AND DISCUSSION

Steady-State Performance

The operating points of the controlled engine in steady state are shown on the diffuser performance map in figure 12. The figure is presented to indicate the variation in diffuser operating point that resulted when a given control was subjected to a range of simulated flight conditions. No comparison of the controls with respect to diffuser pressure ratio at a given flight condition is intended.

The operating points of Δp_I control are shown in figure 12 for both zero and 10° angles of attack. These points show the effects of

the variation in shock position incurred by the use of a constant reference throughout the range of Mach numbers. At Mach numbers of 1.50 and 1.60, the diffuser operated closer to critical pressure ratio than at the higher Mach numbers. (The pressure-ratio peaks represent the critical points at Mach numbers of 1.98 and 1.79; critical operation at a Mach number of 1.50 and zero angle of attack occurs at a temperature ratio of 3.87.) The diffuser operated at 94.5 percent of the critical pressure ratio at a Mach number of 1.50 (zero angle of attack) in comparison with 86.0 percent at a Mach number of 1.98.

The references for Δp_{II} and Δp_{III} controls were reset at a Mach number of 1.50 (as previously stated in the discussion of CONTROL PRINCIPLES) in order to maintain a more constant shock position over the range of Mach numbers. Figure 12 shows that, with Δp_{II} control, the engine operated slightly closer to critical pressure ratio at a Mach number of 1.79 than at a Mach number of 1.98; at a Mach number of 1.50 critical operation was obtained with the reset reference. With Δp_{III} control the engine was held slightly subcritical at all Mach numbers.

The performance of the controlled engine in relation to propulsive thrust and specific fuel consumption is presented in figure 13. The shift in shock position with Δp_I control between Mach numbers of 1.79 and 1.50 noticeably affected engine performance. A greater thrust coefficient and a lower specific fuel consumption were obtained with this control at a Mach number of 1.50 than at a Mach number of 1.79. The engine performance over the Mach number range for Δp_{II} or Δp_{III} control represents a nearly constant shock position.

The results presented in figures 12 and 13 show that the controlled engine performed in steady state as was expected from an examination of the Δp-reference relations in figure 3. When a range of Mach numbers near the design value of the diffuser was covered, a constant reference was sufficient to give a nearly constant shock position. At Mach numbers appreciably below design, however, a shift in shock position resulted with a constant reference (Δp_I control). A nearly constant shock position was maintained over the range of Mach numbers by resetting the reference at the low Mach number for Δp_{II} and Δp_{III} controls.

Automatic variation of the control reference in flight, therefore, appears necessary if a shock-positioning control is to be used to maintain a constant shock position over a wide range of flight conditions. In addition to Mach number changes, large altitude variations will prohibit use of a constant pressure reference. A suggested method to provide a variable reference is to require the control to maintain a constant ratio between the pressures sensed by the two control taps rather than a constant difference. This could readily be done by multiplying the

upstream pressure by a constant factor and using this signal as the reference setting for the downstream pressure. Such a reference would be compensated for altitude changes and, in addition, would provide some Mach number compensation. Proper selection of the constant may provide a suitable reference for the specific Mach number variation of a given flight plan.

A proposed application of this concept to position the shock at the design location used with Δp_{II} control is shown in figure 14. The ratio of the controlled variable p_c to the reference setting $1.35p_a$ is shown as a function of total-temperature ratio for three Mach numbers. The theoretical control point for each Mach number is the intersection of the curve with the dashed line at unity value of the ordinate. Figure 14 can be used with figure 12 to predict the operating points on the diffuser performance map. The diffuser pressure ratios predicted are 97.0 percent and 97.5 percent of the peak values at Mach numbers of 1.98 and 1.79, respectively. In comparison, Δp_{II} control yielded a shift of operating point from 97.0 percent at a Mach number of 1.98 to 99.5 percent of peak pressure ratio at a Mach number of 1.79. A shift in shock position, however, would result with the proposed control at a Mach number of 1.50. At this extreme off-design Mach number, subcritical operation at a temperature ratio of 4.25 is predicted. This shift in shock position, though, would be less than would have resulted with Δp_{II} control if the reference had not been reset. (The theoretical control point at a Mach number of 1.50 for Δp_{II} control before the resetting of the reference was at a temperature ratio of 4.75.)

Effect of Control Settings on Response and Stability

The foregoing discussion was concerned with problems associated with positioning the shock in steady state. A ram-jet control must also be capable of minimizing departures from the specified engine operation during transients imposed on the system by external or internal disturbances. The expected dynamic performance of the control may even influence the selection of the engine operating point for a given application. The dynamic performance attained with each of the three shock-positioning controls is presented in the remainder of the report.

The control action, as previously stated, was proportional-plus-integral, and both the gain of the proportional action and the integrator time constant could be varied. The effect of these controller settings on the dynamic behavior of the three controls was investigated with the simulated flight conditions constant at a Mach number of 1.98 and zero angle of attack.

The response characteristics were determined from transients imposed on the system by fuel-flow disturbances. (The disturbances, as previously explained, were introduced by adding step functions to the fuel servo input voltage.) Response time and overshoot were used as response criteria. Both were measured on the recording of the input voltage to the fuel servo. Response time is defined as the time from the start of the disturbance to the time when 90 percent of the error is eliminated. Overshoot is expressed as the percentage of the disturbance magnitude reached in the first overshoot. In order to illustrate the criteria, a typical transient response is shown in figure 15. This figure shows the response of Δp_I control to a disturbance in fuel flow of about 21 percent of the value corresponding to the control set point. The controller was set to give a loop gain K_L of 0.190. Loop gain is defined as the product of all the gains around the loop, including the gain K of the proportional-plus-integral controller action. (Engine gain was taken at the reference point.) The integrator time constant τ was 0.02 second. The response time for this transient was 0.29 second, and the overshoot was 9.4 percent. The response time included a dead time of about 0.03 second in the response of the controlled variable to fuel flow.

The stability of the control system was investigated by varying the controller settings in steady state. Control reactions to engine noise resulted in small oscillations in the stable region. These oscillations were not sustained in amplitude, and the frequency of oscillation was irregular. Such oscillations are called "irregular oscillations," and the maximum amplitudes and the most predominant frequencies are presented. Amplitude is defined to be one-half of the peak-to-peak variation during a cycle. Oscillations that indicated system instability were sustained in amplitude, and the frequencies were nearly constant when loop gain was varied.

Δp_I Control. - The effect of loop gain and integrator time constant on the dynamic performance of Δp_I control is presented in figures 16(a) and (b), respectively. Response time, overshoot, and stability characteristics are shown in figure 16(a) as functions of loop gain for an integrator time constant of 1.0 second. The same performance parameters are shown as functions of the reciprocal of the integrator time constant at loop gains of 0.095 and 0.190 in figure 16(b). The response data are given for both positive and negative fuel-flow disturbances of 556 pounds per hour (21 percent of the value required in steady state by the control).

The response of the control-engine combination was dependent on the sign of the disturbance in fuel flow. For this control, the smaller response times were obtained for disturbances that increased fuel flow. An explanation of this result is suggested by the steady-state relation

of the controlled variable to fuel flow (fig. 3). On the basis of this relation, a positive disturbance of 556 pounds per hour would result in an error from the set point of 970 pounds per square foot absolute, whereas an equivalent negative disturbance would produce an error of only 150 pounds per square foot absolute. A larger error, of course, results in greater corrective action by the control.

Since the integrator time constant was large, the responses represented by the data of figure 16(a) were greatly overdamped. The response times were long, and no overshoot occurred. The data were taken primarily to indicate the stability limit that might be expected if a pure proportional control was used. The integrator time constant of 1.0 second was sufficiently large to provide stability information approaching that from a proportional control. The variation of oscillation amplitudes shown in the figure indicates that the loop gain for instability is about 0.7, and the frequency of oscillation is 8.8 cycles per second. For faster integrator action, the control system would become unstable at a lower value of loop gain. The rather low value of loop gain (0.7) for instability is the result of an over-all amplitude-frequency characteristic that has a gain greater than unity at the frequency of instability (8.8 cps). This peaking of the over-all amplitude-frequency characteristic appears to be a result of the fuel-system response obtained for this control. The frequency-response performance that was previously presented for the fuel system (fig. 10) was not attained with Δp_I control. At the relatively small fuel flows involved, the manifold pressures were too low for fast response of fuel flow to fuel valve position.

Faster response, of course, was achieved with Δp_I control as the integrator action was made more rapid. Figure 16(b) shows the decrease in response time obtained by increasing the integrator rate at constant loop gains. The fastest control response was recorded for a reciprocal integrator time constant of 100 (1/sec) with loop gain at 0.190. The response time for this positive disturbance in fuel flow was 0.15 second, and the overshoot was 18 percent. The same control settings also gave stable operation. The oscillation in steady state was irregular at about 4 cycles per second, and the maximum amplitude in fuel flow was 35 pounds per hour. Considered in relation to diffuser operating point, the oscillation in diffuser pressure ratio was less than ± 0.5 percent of the steady value corresponding to the control set point.

A response time less than the minimum shown in figure 16(b) can be expected with higher loop gain. With a reciprocal integrator time constant of 100 (1/sec), the response time was halved when the loop gain was increased by a factor of 2. A further decrease in response time, therefore, should result from higher loop gains than those employed. This improvement, of course, would be coupled with an increase in overshoot.

A limiting value of response time, however, is imposed by the dead time of the over-all system (dead time of the controlled pressure plus the effective dead time of the fuel system). A response time equal to this dead time is the theoretical minimum. The value of system dead time calculated on the basis of 180° phase shift at 8.8 cycles per second is 0.057 second. This calculated value compares favorably with values of system dead time of 0.035 to 0.05 second, which were experimentally determined from engine and fuel-system dynamics.

Δp_{II} Control. - The effect of loop gain and integrator time constant on the response and stability of Δp_{II} control is presented in figures 17(a) and (b), respectively. The performance criteria are shown as functions of loop gain in figure 17(a) for an integrator time constant of 0.1 second. The variation of these criteria with reciprocal integrator time constant for a loop gain of 1.16 is shown in figure 17(b). The positive and negative fuel-flow disturbances were 278 pounds per hour in magnitude (8.4 percent of the value required in steady state by the control).

The response of Δp_{II} control was faster for negative disturbances in fuel flow than for positive. This result is a reversal of that for Δp_I control. The error in the controlled variable was greater this time in the negative direction for the 278-pound-per-hour disturbance (fig. 3). The error, or restoring signal, for the negative disturbance was also maintained at its initial value for almost two-thirds of the fuel-flow recovery.

The minimum response time obtained with Δp_{II} control was nearly equal to the dead time of the system. Figure 17(a) shows that this minimum response time (0.05 sec) was measured for a loop gain of 6.96. The oscillations in steady state, though, were sustained. At this loop gain, the frequency of oscillation was 9 cycles per second, and the amplitude in fuel flow was 175 pounds per hour. The oscillation amplitude of diffuser pressure ratio, however, was only 1.9 percent of the steady value. The data of figure 17(a) indicate that the stability limit for this integrator setting was reached when the loop gain was about 2.5. Frequency-response data for the system components substantiated this value of stability limit. With this control, the fuel-system response was comparable with the response shown in figure 10.

When small integrator time constants were used in combination with a loop gain of 1.16, the control responded rapidly, and the system was stable (fig. 17(b)). A reciprocal integrator time constant of 100 (1/sec) gave a response time of 0.08 second with an overshoot of 98 percent (negative disturbance). With the same control settings, the oscillations in steady state were irregular with an amplitude of 80 pounds per hour in fuel flow. The amplitude of diffuser pressure ratio was 1.0

percent of the steady value. Response times for the negative disturbances were only slightly greater than 0.08 second at values of the reciprocal integrator time constant smaller than 100, and the overshoot was considerably less with the slower integrator action. The faster integrator rate, however, would be advantageous in avoiding subcritical operation of the engine. In this regard, the response time to positive disturbances is the important consideration.

Δp_{III} Control. - The dynamic performance of Δp_{III} control with various controller settings is presented in figure 18. Figure 18(a) shows the effect of loop gain on the response and stability for an integrator time constant of 0.1 second. The criteria are shown in figure 18(b) as functions of the reciprocal integrator time constant for a loop gain of 2.40. The disturbance size was ±278 pounds per hour of fuel flow (7.9 percent of the value required in steady state by the control).

This control responded faster for the negative disturbances, as did Δp_{II} control. Since both controlled the engine near critical, this characteristic was not desirable. More rapid response to positive disturbances could be expected if these controls were referenced to smaller values of the differential pressures. A larger potential error would then exist in the positive direction (fig. 3), and for Δp_{II} control the rate of change of the controlled variable with fuel flow would be more favorable near the reference point.

The most rapid response with a stable system was obtained with a loop gain of 2.40 and a reciprocal integrator time constant of 70 (1/sec) (fig. 18(b)). The response time for the negative disturbance was 0.09 second, and the overshoot was 35 percent. For the positive disturbance, a response time of 0.15 second was obtained for a transient with 17-percent overshoot. With these control settings, the fuel flow oscillated irregularly in steady state with an amplitude of 40 pounds per hour. The oscillation in diffuser-exit total pressure gave a pressure-ratio amplitude equal to 1.2 percent of the steady value.

When the reciprocal integrator time constant was increased to 100 (1/sec) with a loop gain of 2.40, the system became unstable (fig. 18(b)). A sustained oscillation existed at 6 cycles per second. The fuel-flow amplitude, though, was just 80 pounds per hour; the diffuser pressure-ratio amplitude was 1.7 percent of the steady value. The instability at this integrator rate indicates that the loop gain used was close to the stability limit for nearly proportional control. The conclusion is substantiated by figure 18(a), which shows that a loop gain greater than 2.40 gave instability with a low integrator rate.

Summary remarks. - The foregoing results have shown that, when relatively small disturbances were imposed on each of the three controls, the

responses were very similar. Satisfactory stable responses with short response times were obtained with all three controls. With proper adjustment of the control settings, response times less than 0.1 second could be attained within the stable region of each control. Such response times were obtained with an integrator time constant near 0.01 second and with loop gain within 50 to 100 percent of the gain required for instability. The minimum response time attained (0.05 sec) was nearly equal to the system dead time. This response time of 0.05 second was obtained with control settings beyond the stability limit, but the amplitude of the resulting oscillation was not excessive.

Effect of Disturbance Size and Mach Number on Response to Fuel-Flow Disturbances

The effect of the disturbance magnitude on the response of Δp_I control to a fuel-flow disturbance is presented in figure 19. The figure shows response time as a function of disturbance magnitude for engine operation at a Mach number of 1.98 and zero angle of attack. The constant control settings were: loop gain, 0.286; integrator time constant, 0.02 second. The response time lengthened as the magnitude of the disturbance was increased for both the positive and negative disturbances, but more markedly for the negative. This difference was caused by the saturation (limiting) of the pressure error in the negative direction. The same error magnitude was produced by each of the negative disturbances. Response time increased from 0.17 second to 0.65 second as the negative disturbances were increased in magnitude from 278 to 1390 pounds per hour (about 11 to 54 percent of the fuel flow in steady state). An equivalent range of positive disturbances increased the response time from 0.16 second to 0.265 second.

The response times of Δp_{II} and Δp_{III} controls also increased when the disturbance magnitude was increased, but the amount of the increase was similar for both positive and negative disturbances. With these controls, the potential error signals were approximately equal in both the positive and negative directions. The rates at which response time increased with Δp_{II} and Δp_{III} controls were only slightly greater than that shown in figure 19 for positive disturbances with Δp_I control.

The effect of Mach number on response time is presented for Δp_I control in figure 20. Response time for a fuel-flow disturbance of ± 278 pounds per hour is shown as a function of Mach number for constant controller settings. The integrator time constant was 0.02 second. Loop gain varied, since the engine gain changed with Mach number; the loop gain became less as the Mach number decreased. The loss in loop gain, of course, tended to increase the response time at the lower Mach numbers.

The figure shows that, for the positive disturbances, the response time increased almost linearly with decrease in Mach number from 1.98 to 1.50. When the disturbance was negative, however, the response time was nearly constant for Mach numbers of 1.98 and 1.79; a longer response time was obtained only at a Mach number of 1.50. Although the response times were nearly equal for the two disturbances at a Mach number of 1.98, the negative disturbances gave faster responses than did the positive disturbances at the lower Mach numbers. These results indicate that the responses were not solely affected by the decrease in loop gain. In addition, the responses at a given Mach number were dependent on the nature of the Δp variation above or below the reference setting.

Mach Number Disturbances

The results presented in the remainder of the report were not necessarily obtained with optimum control settings. They do, however, provide information indicative of the control capabilities.

The Mach number disturbances were, in general, not fast enough to impose noticeable errors from the set point during the transients. Figure 21 shows a transient record for a disturbance in Mach number in which engine operation was closely controlled throughout the transient. The control was Δp_I with the following settings: loop gain, 0.262 (Mach number of 1.79); integrator time constant, 0.02 second. The change in Mach number, which was accomplished in about 0.6 second, was from 1.84 to 1.79 and is represented in the figure by the concurrent transient in free-stream static pressure. This accompanying transient was a consequence of the technique used to disturb Mach number. The combined disturbance subjected the controlled engine to a simulated altitude decrease in addition to the Mach number transient. In order to correct for the disturbance, the control had to increase fuel flow. The corrective action was rapid in relation to the disturbance rate: No readable change in the controlled variable was recorded during the transient.

When the disturbances in Mach number included the diffuser "starting" Mach number, a noticeable error was imposed on the control system in the transient. Starting refers to the minimum Mach number at which the diffuser internal flow could be supersonic upstream of the throat. Two disturbances which included this Mach number are shown in the transient records in figure 22. The control was Δp_I; the controller settings were the same as for the Mach number disturbance discussed previously. The disturbances in figure 22, however, were more severe. When the transient Mach number became equal to the starting value, the change in the internal flow of the diffuser was abrupt. The controlled pressure differential, therefore, was subjected to a faster disturbance than was associated with the other Mach number changes. Figure 22(a) shows the transient error which resulted from the sudden start of supersonic flow in the inlet

during a transient in Mach number from 1.67 to 1.77. A disturbance that decreased the Mach number through the starting value is shown in figure 22(b). A noticeable error appeared in the controlled variable when the inlet flow became subsonic. Both errors, however, were reduced to zero in approximately 0.3 second, and more optimum control settings would reduce the duration of the errors.

Angle-of-Attack Disturbances

A transient record of an angle-of-attack disturbance with Δp_I control is presented in figure 23. With the Mach number at 1.98, the angle of attack was changed from zero to 10° in about 1.0 second. The controller gain had been set to provide a loop gain of 0.286 at zero angle of attack, and the integrator time constant was 0.02 second. During the transient, the control decreased fuel flow quickly enough to keep the controlled variable practically equal to the reference setting throughout the disturbance. At the end of the transient, the engine fuel flow was approximately 100 pounds per hour less than at zero angle of attack. The Δp_I control performed similarly to disturbances in angle of attack at Mach numbers of 1.79 and 1.50.

When the engine, controlled by Δp_{II}, was pitched from zero to 10° at a Mach number of 1.98, subcritical operation with severe buzz and subsequent combustion blow-out occurred at the end point of the transient. An attempt to operate the engine manually in the subcritical region with an angle of attack of 10° at a Mach number of 1.98 also resulted in blow-out and showed this to be an inoperable region of the engine. It should be emphasized that the departure into the subcritical region with the control was not due to the response of the control. The engine was closely controlled to the set point during the transient, but this set point corresponded to subcritical operation at a 10° angle of attack. At this angle of attack, the shock was canted with respect to the diffuser axis in such a way that the controlled pressure differential (Δp_{II}) was equal to the reference setting when the upper portion of the shock was ahead of the inlet lip. (The pressure taps used were in the horizontal plane through the diffuser axis.)

Because of the blow-out difficulties at a Mach number of 1.98, further investigations of transients in angle of attack were made at a Mach number of 1.77. Both Δp_{II} and Δp_{III} controls performed satisfactorily at this Mach number during transients from zero to 10° angles of attack. The controlled engine was again subcritical at the end points of the transients; such operation, however, did not result in blow-out at this Mach number.

The angle-of-attack transients with Δp_{II} and Δp_{III} controls showed that, if near-critical operation of the ram jet is required (at zero angle of attack), the control will have to be compensated for angle of attack if it is necessary to avoid subcritical operation and its attendant buzz when angle of attack is encountered. Adequate compensation might be provided by incorporating auxiliary pressure taps into the system in such a way that they will give an error signal to the control when a portion of the shock is external. Two auxiliary taps at the inlet, one on the upper surface of the centerbody and one on the lower surface, may be sufficient to compensate a near-critical control (such as Δp_{II}) for both positive and negative angles of attack. The pressures sensed by these auxiliary taps could readily be referenced to provide an error signal only for subcritical operation.

Exhaust-Area Disturbances

Transients with Δp_I control resulting from rapid changes in exhaust area at a Mach number of 1.77 are shown by the recordings in figure 24. The controller was set to give a loop gain of 0.262 at the initial area of 0.960 square foot; the integrator time constant was 0.02 second. The transient presented in figure 24(a) was caused by a decrease in exhaust area from 0.960 to 0.864 square foot, while figure 24(b) shows the transient which resulted when the area was returned from 0.864 to 0.960 square foot. With the controller settings employed, the rates at which the disturbances were imposed were sufficient to cause transient errors to appear in the recordings of the controlled variable. The departure of the diffuser-exit total pressure from its steady-state value, however, was not excessive. The maximum variation was 2.6 percent of the value in steady state for the area decrease and 4.2 percent for the area increase. The increase in exhaust area, of course, corresponded to a negative disturbance in fuel flow, for which early saturation of the error signal occurred with this control. The area disturbances, which were 10 percent of the original area in magnitude, required fuel-flow corrections of approximately 500 pounds per hour to return the engine to the set point of the system.

Exhaust-area disturbances of 21 percent of the original area (0.960 sq ft) were made at a Mach number of 1.98 and are presented in figure 25. These disturbances corresponded in magnitude to fuel-flow disturbances of about 1200 pounds per hour. The engine was controlled by Δp_{II}. Loop gain was 2.32 for an exhaust area of 0.960 square foot, and the integrator time constant was 0.033 second. The disturbance shown in figure 25(a) decreased the area to 0.755 square foot in 0.14 second. The diffuser shock was expelled during the transient, and, as a result, the recovery had to be accomplished in the presence of considerable pressure

pulsing. The control, however, functioned satisfactorily during the oscillations and decreased fuel flow in a nearly linear manner while the engine operated in the subcritical region. The time spent in subcritical operation (0.4 sec) is indicated in the figure by the record of the diffuser-lip pitot pressure. The return disturbance is shown in figure 25(b); the area change again was made in 0.14 second. The behavior of the controlled variable indicated that, during the transient, the shock moved downstream of the design position and supersonic flow existed at both pressure taps of the control. The resultant saturation of the error signal was, of course, detrimental to the control response. The shock, however, did not move far enough for the flow to be supersonic at the station where the downstream tap of the Δp_I signal was located. The total recorded time for operation off the set point was approximately 0.46 second.

Recovery From Subcritical Engine Operation

As stated previously, many ram-jet engines display severe pulsing characteristics called buzz when operated subcritically. Violently pulsing pressures may cause combustion blow-out or structural damage. The control, therefore, must respond quickly enough to prevent buzz or to minimize its duration when disturbances tend to cause subcritical operation.

The performance of the controls in relation to the above requirement was investigated at a Mach number of 1.98 and zero angle of attack. The investigation was made by imposing, on each control, fuel-flow disturbances of sufficient magnitude to exceed the fuel flow for well-defined buzz in steady state (about 3520 lb/hr at this flight condition). Well-pronounced buzz existed for steady-state operation of the engine in the major portion of the subcritical region at this flight condition. Fifteen cycles per second was the predominant buzz frequency for moderate subcritical operation. Extreme subcritical operation resulted in 200-cycle-per-second oscillations of large amplitude modulated at 15 cycles per second. No well defined buzz, however, existed for slight subcritical operation: Oscillograms for Δp_{III} control in steady state showed that, although pulsing was present in the inlet, the oscillations were irregular and attenuated at the diffuser exit.

The Δp_I control, which had a large operating margin from the buzz region in steady state, recovered from each disturbance with no diffuser buzz. The control settings used for each disturbance were: loop gain, 0.286; integrator time constant, 0.02 second. The transient response for the largest disturbance is shown in figure 26(a). The disturbance magnitude was 1390 pounds per hour (2600 to 3990 lb/hr). Although no buzz was recorded, the engine operated subcritically for 0.09 second during the transient.

The Δp_{II} control, which had only a small operating margin from the buzz region in steady state, recovered without engine buzz for the smallest disturbance but not for larger ones. The loop gain was 2.32 and the integrator time constant was 0.033 second for each disturbance. No buzz was recorded for the disturbance from 3300 to 3578 pounds per hour, although the engine was subcritical for 0.055 second. The response time was 0.245 second. Disturbances of 556 pounds per hour and larger resulted in buzz. The transient response to the disturbance of 556 pounds per hour is shown in figure 26(b). Both the low and high frequencies of buzz are evident in each pressure record. The subcritical time for this transient was 0.17 second.

The Δp_{III} control, as stated previously, held the engine in mild buzz in steady state, and all the disturbances gave more definite buzz in the transients. The response to the 278-pound-per-hour disturbance (3520 to 3798 lb/hr) is shown in figure 26(c). The control settings for this disturbance were: loop gain, 2.40; integrator time constant, 0.02 second. During this transient, oscillations at 15 cycles per second were recorded in the diffuser-exit total pressure. For the largest disturbance (1390 lb/hr), a response time of 0.31 second was attained in the presence of severe buzz.

Diffuser operating conditions during a transient into the subcritical region without buzz are compared in figure 27 with those for a transient in which buzz occurred. The transient, with Δp_I control, imposed by a disturbance of 1390 pounds per hour (fig. 27(a)) is compared with the transient with diffuser buzz which resulted from a disturbance of 834 pounds per hour on Δp_{II} control (fig. 27(b)). The figure shows the transient relations of diffuser pressure ratio to fuel flow. Time from the beginning of the disturbance in fuel flow is noted for the interesting points. Figure 27(a) shows that the engine operation became subcritical 0.05 second after the fuel-flow disturbance with Δp_I control. With Δp_{II} control, however, the shock was expelled at 0.04 second (fig. 27(b)). This difference, of course, resulted because the set point for Δp_I control was more supercritical; thus, a greater pressure change and, hence, longer time was required to expel the shock. (Engine dynamics data indicated that the pressure change to a fuel-flow disturbance was, in general, lead-lag in nature after the dead time.) Fuel-flow reduction began at 0.04 second with Δp_I control and at 0.045 second with Δp_{II} control. By adding to these times the dead time between a decrease in fuel flow and the resultant pressure change at the diffuser inlet (0.035 sec), the time for the initiation of shock recovery is found to be 0.075 second for Δp_I control and 0.080 second for Δp_{II} control. Shock recovery with Δp_I control, therefore, started 0.025 second after the shock was expelled. With Δp_{II} control, however, the shock had been external for 0.04 second and buzz had already commenced at the time shock recovery was begun.

The preceding discussion has emphasized that it may be difficult to completely avoid buzz when controlling near the critical point. This difficulty primarily results from the short time for shock expulsion in relation to the dead times involved. A margin of operation from the buzz region in steady state, therefore, may be required if an engine displaying severe buzz characteristics is to be adequately controlled.

Figure 27, however, suggests how a near-critical control (such as Δp_{II}) might be improved in its ability to keep the time in buzz at a minimum. The figure shows that in the initial stages of recovery Δp_I control decreased fuel flow at a much faster rate than did Δp_{II} control. The faster action of Δp_I control primarily resulted from a larger restoring signal from the controlled variable. At the critical point, the Δp_I pressure error was about twice as large as the Δp_{II} pressure error. The Δp_{II} control could be provided with a greater error signal for subcritical transients by the addition of a high-gain limiter to the control system. The controlled variable used for Δp_{III} control, for example, could provide a limiting signal for Δp_{II} control. The control system discussed in reference 7 used the Δp_{III} pressure signal as a limiting control. Another method that might be used to speed recovery from subcritical operation is the variation of controller settings with error signal to provide faster control action for positive than for negative errors. Stability requirements, however, may necessitate the scheduling of a specific value of positive error to actuate this change in controller settings.

SUMMARY OF RESULTS

Ram-jet-engine control by shock positioning has been demonstrated with a continuous-acting, closed-loop system utilizing proportional-plus-integral control action over a Mach number range of 1.50 to 1.98, pressure altitudes of 26,500 to 36,500 feet, and at zero and 10° angles of attack. Three design positions of the shock (well supercritical, near critical, and slightly subcritical) were investigated. The salient results of the investigation are summarized as follows:

1. Shock positioning appears to be a practical way to control the operation of the ram jet.

2. Operation over a wide range of flight conditions requires a variable control reference: Simple automatic compensation of the reference for altitude changes (and for limited Mach number changes) appears possible.

3. A near-critical control must be compensated for angle of attack if it is necessary to avoid subcritical operation of the engine.

4. Satisfactory stable responses with response times less than 0.1 second were obtainable for each of the three design positions of the shock. Such responses were attained with an integrator time constant near 0.01 second and with loop gain within 50 to 100 percent of that required to produce instability. The minimum response time (0.05 sec) was nearly equal to the system dead time.

5. In order to avoid diffuser buzz during transients, it was necessary to provide some operating margin in steady state from the buzz region. When no such margin was provided (the slightly subcritical position of the shock), well-pronounced buzz occurred in the transient whenever a positive disturbance in fuel flow was imposed. With a large margin (the well-supercritical position of the shock), the control recovered with no diffuser buzz even when fuel flow was disturbed to extremely subcritical values. Engine performance in steady state, however, was sacrificed with this large margin. A small margin (the near-critical position of the shock) gave the best compromise between engine performance in steady state and protection from diffuser buzz during transients. With the near-critical shock position, small transients into the steady-state region of buzz were made without incurring buzz. Buzz did occur during large transients, but the control rapidly restored the engine to the desired operating point.

Lewis Flight Propulsion Laboratory
National Advisory Committee for Aeronautics
Cleveland, Ohio, June 24, 1955

APPENDIX A

SYMBOLS

The following symbols are used in this report:

A	area
C	capacitance
C_{F-D}	coefficient of propulsive thrust, $\frac{F - D}{q_O A_{max}}$
D	external drag of engine
F	internal thrust
K	controller gain
K_L	loop gain
M	Mach number
P	total pressure
p	static pressure
q	dynamic pressure, $\frac{\gamma}{2} pM^2$
R	resistance
s	complex operator
sfc	specific fuel consumption, $\frac{w_f}{F - D}$
T	total temperature
V_1	controller input voltage
V_2	controller output voltage or fuel-servo input voltage
V_3	feedback voltage
w_f	fuel flow
α	angle of attack
γ	ratio of specific heats for air

Δp_s pressure drop of secondary-fuel nozzles

Δp_I $p_d - p_b$

Δp_{II} $p_c - p_a$

Δp_{III} $p_b - p_a$

ε error signal

τ integrator time constant

Subscripts:

a diffuser centerbody surface, 4 in. upstream of cowl lip, horizontal plane

b diffuser centerbody surface, in plane of cowl lip, horizontal plane

c diffuser centerbody surface, 6 in. downstream of cowl lip, horizontal plane

d diffuser centerbody surface, 15 in. downstream of cowl lip, horizontal plane

max maximum

x diffuser exit

0 free stream

6 exhaust-nozzle exit

APPENDIX B

INSTRUMENTATION

Engine Variables

For the measurement of engine variables during transient operation of the engine, it was necessary to select instruments having fast response in view of the short response times expected. For the measurement of pressures within the engine, pressure transducers of the variable-inductance type having high natural frequencies were selected. Connecting-tubing lengths were kept to a minimum, and, wherever possible, static pressures were measured by transducers screwed directly into the static-pressure tap.

The response characteristics of the pressure transducers were obtained from bench tests. The step-function response was determined for each transducer and its associated tubing, and a limited number of sinusoidal response tests were made for each type of transducer with several tubing combinations. The response characteristics are tabulated subsequently for each variable. Where reference is made to the frequency-response curves of figures 28 to 30, the data were taken for the specific transducer and tubing used. Where the curve is indicated as (approx.), the comparison of tubing dimensions and the step-function responses shows sufficient agreement to permit use of the specified curves. The accuracy of the step-function data given is limited to approximately 0.5 millisecond in measurement of response time and ±5 percent in overshoot. The step data were recorded with a galvanometer having a natural frequency of 500 cycles per second, damped at 64 percent of critical, which gave a flat response of ±5 percent at frequencies to 300 cycles per second. Since the galvanometer response is the same order of magnitude as the possible error in the measurements, no correction has been made in the data for the effect of the galvanometer.

Variable	Transducer type	Frequency-response characteristic		Response to step function	
		Figure	Curve	Time (63-percent point), sec	Percent overshoot
$\Delta p_I \begin{cases} p_d \\ -p_b \end{cases}$	I	33 33	A C (approx.)	0.0005 .0014	8.6 60.0
$\Delta p_{II} \begin{cases} p_c \\ -p_a \end{cases}$	III	35 --	C ----------	.0072 .072	None None
$\Delta p_{III} \begin{cases} p_b \\ -p_a \end{cases}$	II	34 --	A (approx.) ----------	.0009 .014	25.8 None
p_0	I	33	A	.0005	8.6
p_x	I	33	A	.0005	8.6
P_x	III	35	B	.0041	None
Diffuser-lip pitot pressure	I	33	C (approx.)	.0013	60.0

For steady-state performance and transducer calibration, these pressures were measured by manometers.

Angle of Attack and Area

For the measurement of angle of attack and exit nozzle area during transient, slide-wire potentiometers connected in a resistance bridge circuit were used. The exit-area indication was obtained by sensing the position of the exit plug which reduced the area linearly as it was moved into the nozzle. In steady state these variables were measured by counters.

Fuel Variables

Fuel-nozzle pressure drop was measured by resistance strain-gage-type differential pressure transducers connected approximately 8 inches upstream of both the primary and secondary fuel nozzles and referenced to the air pressure in the region of the nozzles. The response of the fuel pressure side of the transducers with tubing was found from bench tests to be flat within ±5 percent to frequencies of at least 150 cycles

per second with no measurable phase shift. For steady-state measurements, fuel pressures were sensed by autosyn-type pressure transmitters, and fuel flow was measured by rotameters.

The input voltage to the fuel servo and the fuel-valve-position signal were measured directly at the fuel-servo control panel and connected to the recorder by means of isolating d-c amplifiers and matching networks to provide the proper sensitivity and damping characteristics for the galvanometers. The frequency response of the amplifiers was flat within ±5 percent to 200 cycles per second.

Transient Recording

All transient measurements were recorded on sensitized paper in a galvanometric oscillograph with galvanometer elements having natural frequencies of 210 to 500 cycles per second, depending on the amount of filtering desired. In addition, certain variables were monitored on a direct-inking oscillograph having a flat frequency response of 100 cycles per second.

REFERENCES

1. Boksenbom, Aaron S., and Novik, David: Control Requirements and Control Parameters for a Ram Jet with Variable-Area Exhaust Nozzle. NACA RM E8H24, 1948.

2. Himmel, Seymour C.: Some Control Considerations for Ram-Jet Engines. NACA RM E52F10, 1952.

3. Vasu, G., Wilcox, F. A., and Himmel, S. C.: Preliminary Report of Experimental Investigation of Ram-Jet Controls and Engine Dynamics. NACA RM E54H10, 1954.

4. Hearth, Donald P., and Perchonok, Eugene: Performance of a 16-Inch Ram-Jet Engine with a Can-Type Combustor at Mach Numbers of 1.50 to 2.16. NACA RM E54G13, 1954.

5. Fox, Jerome L.: Supersonic Tunnel Investigation by Means of Inclined-Plate Technique to Determine Performance of Several Nose Inlets over Mach Number Range of 1.72 to 2.18. NACA RM E50K14, 1951.

6. Otto, Edward W., Gold, Harold, and Hiller, Kirby W.: Design and Performance of Throttle-Type Fuel Controls for Engine Dynamic Studies. NACA TN 3445, 1955.

7. Dunbar, William R., Vasu, George, and Hurrell, Herbert G.: Experimental Investigation of Direct Control of Diffuser Pressure on 16-Inch Ram-Jet Engine. NACA RM E55D15, 1955.

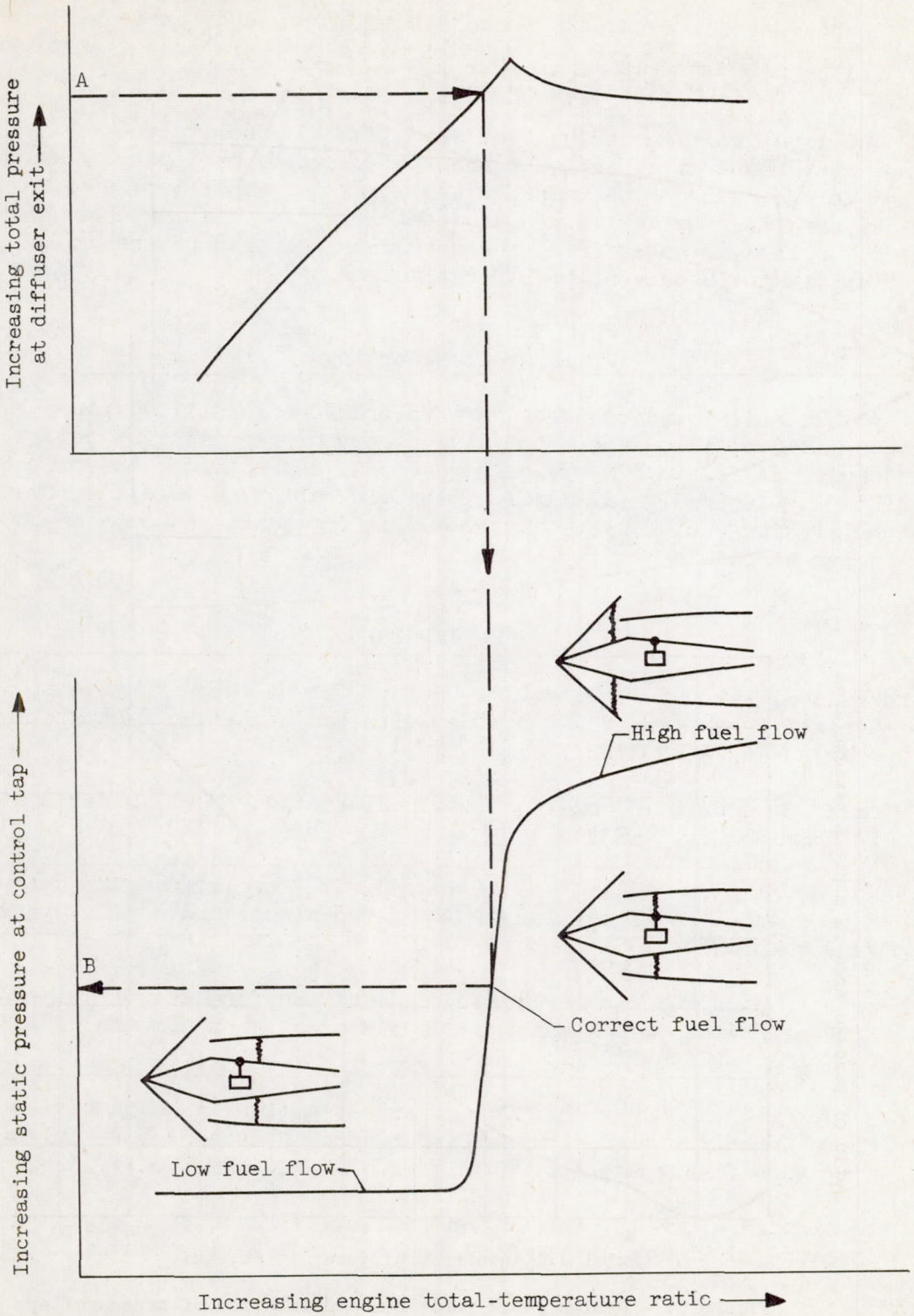

Figure 1. - Illustration of control principle. Flight conditions constant.

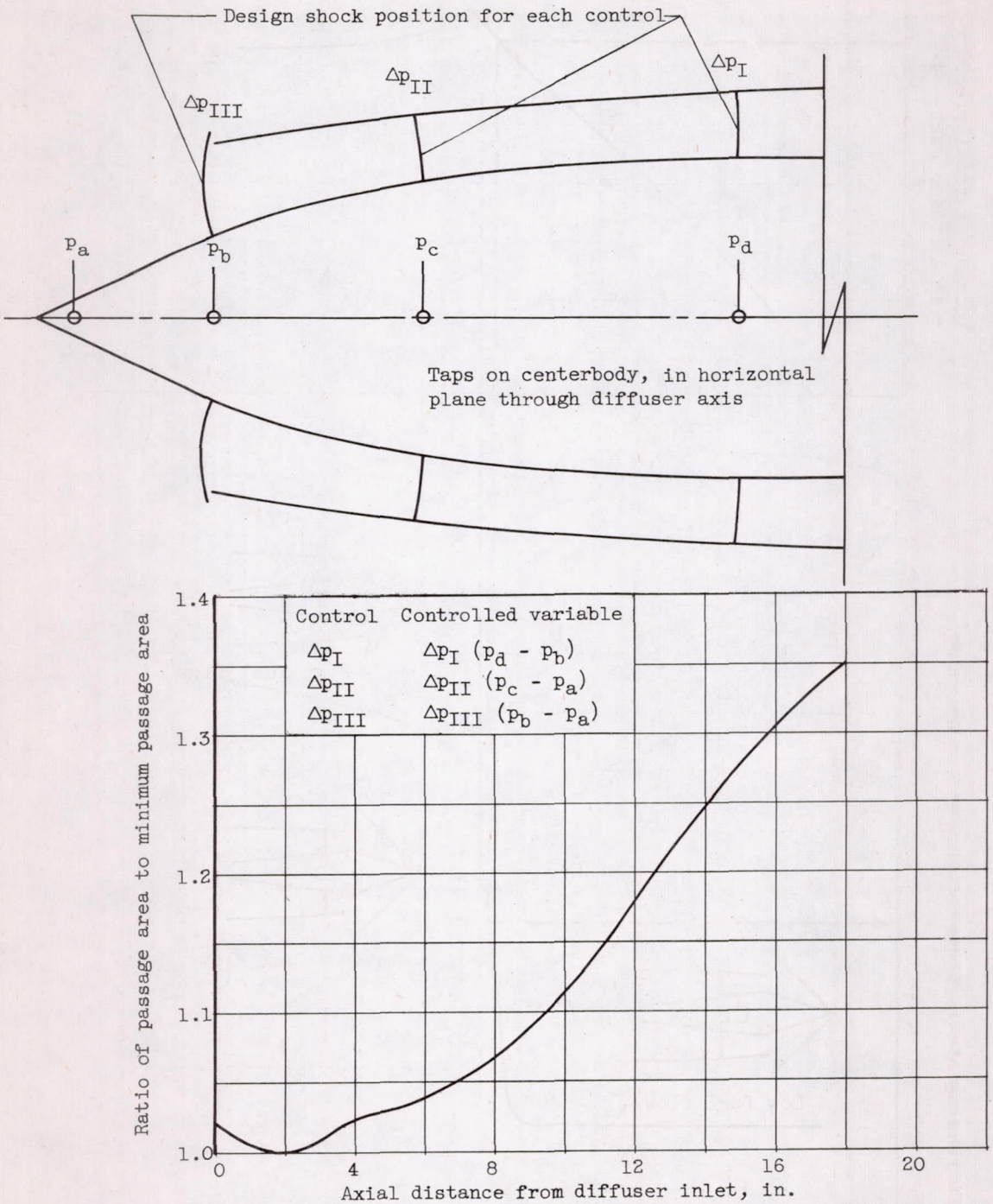

Figure 2. - Design shock positions and location of pressure taps used in control system.

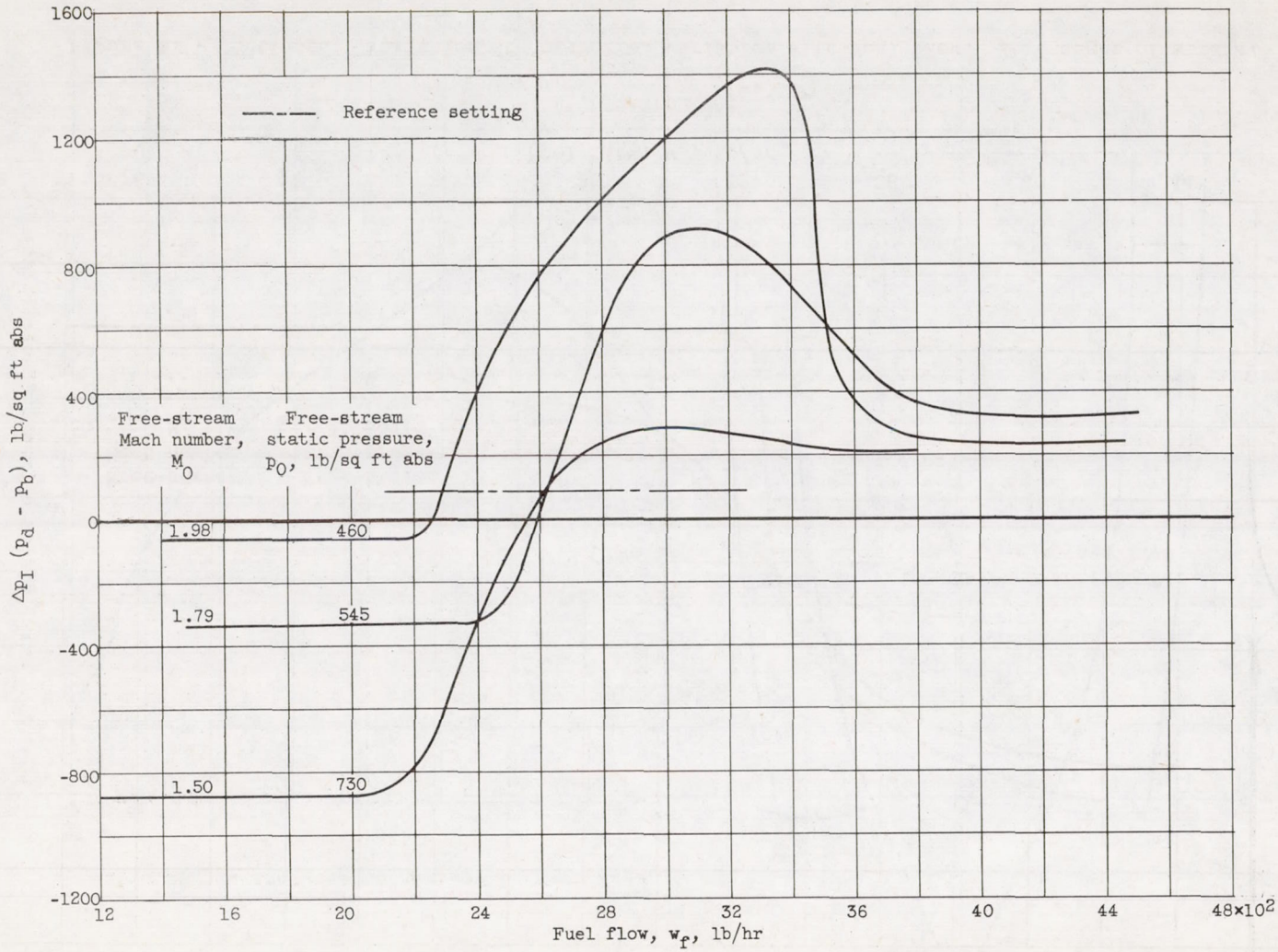

(a) Control, Δp_I.

Figure 3. - Variation of controlled variables with fuel flow. Zero angle of attack.

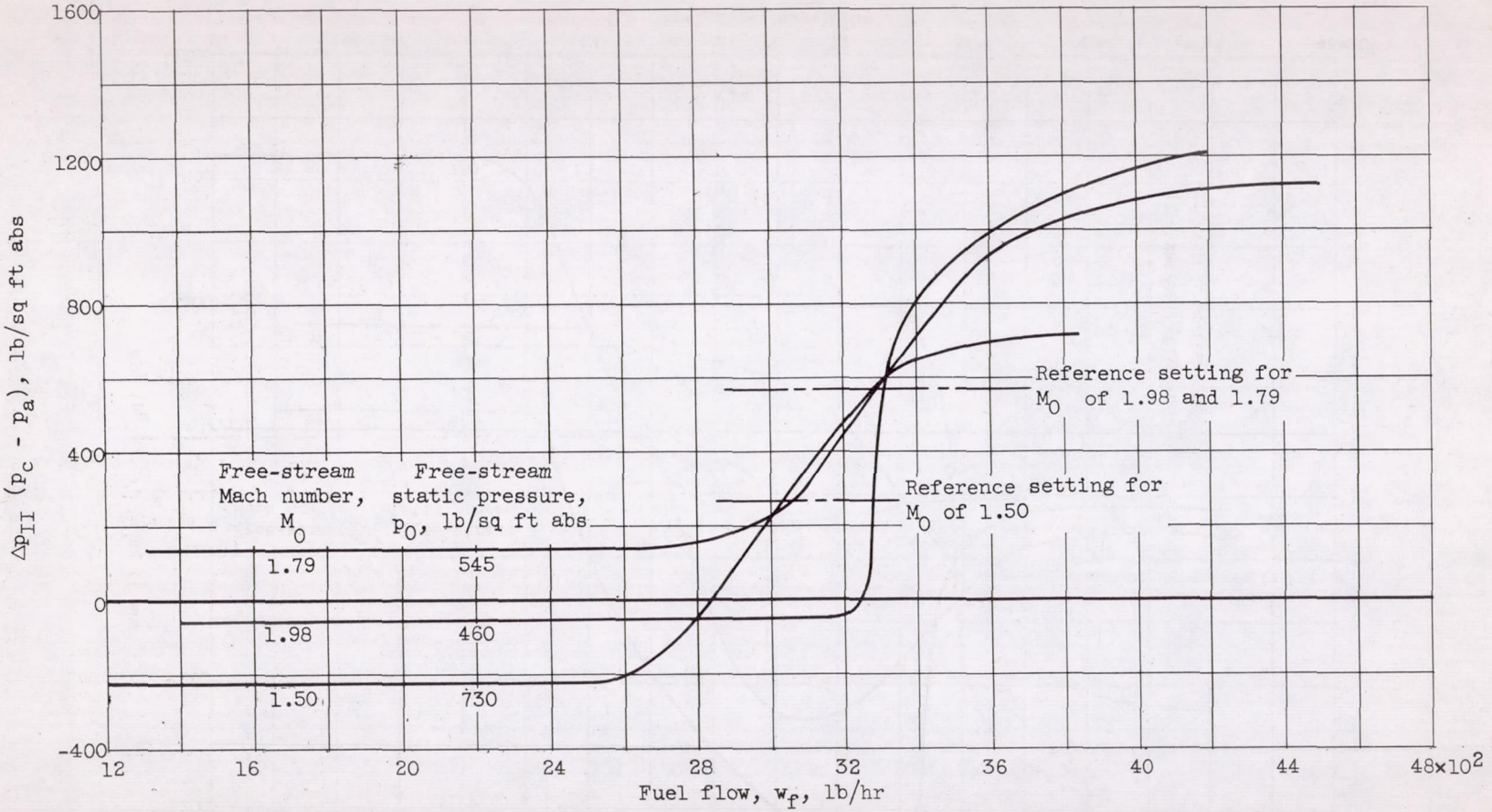

(b) Control, Δp_{II}.

Figure 3. - Continued. Variation of controlled variables with fuel flow. Zero angle of attack.

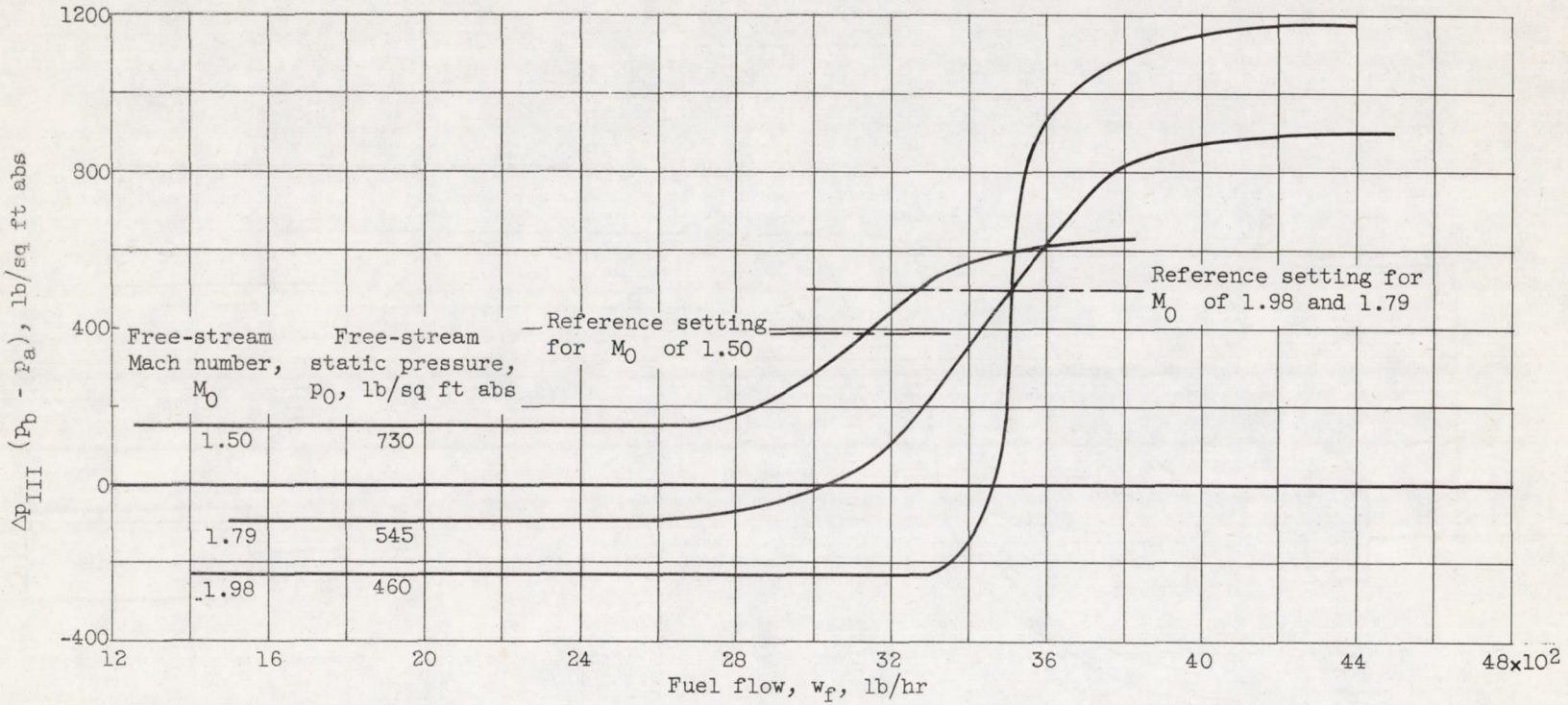

(c) Control, Δp_{III}.

Figure 3. - Concluded. Variation of controlled variables with fuel flow. Zero angle of attack.

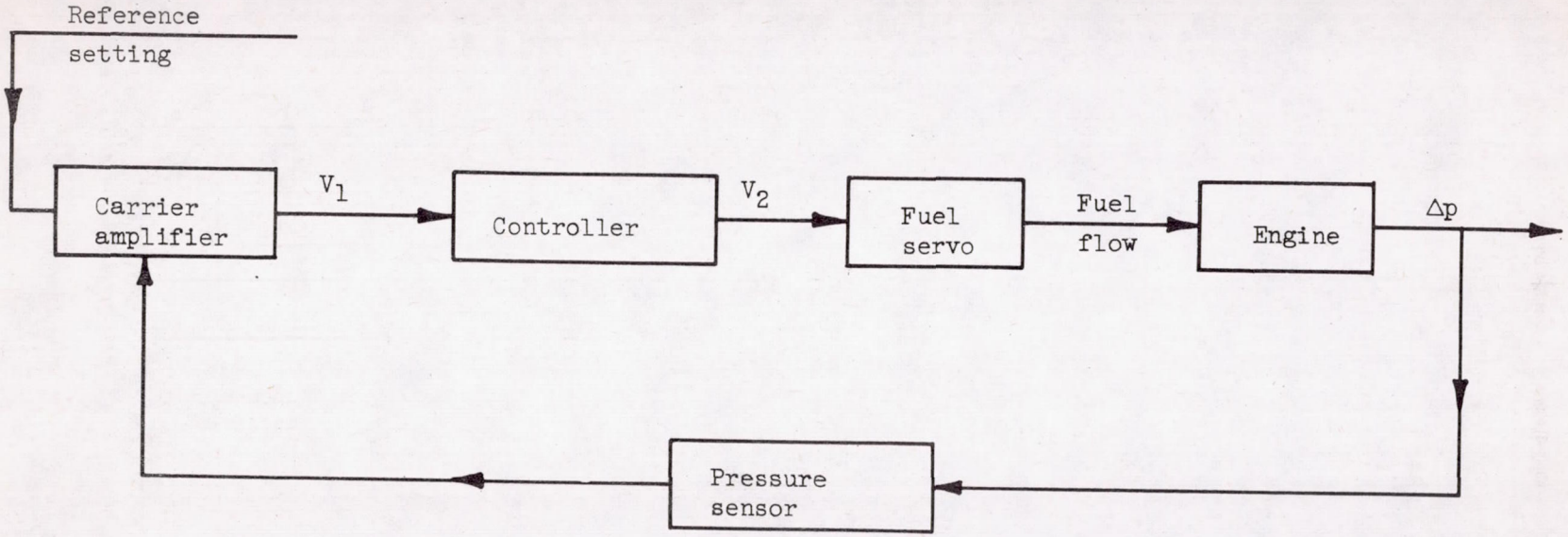

Figure 4. - Block diagram of control system.

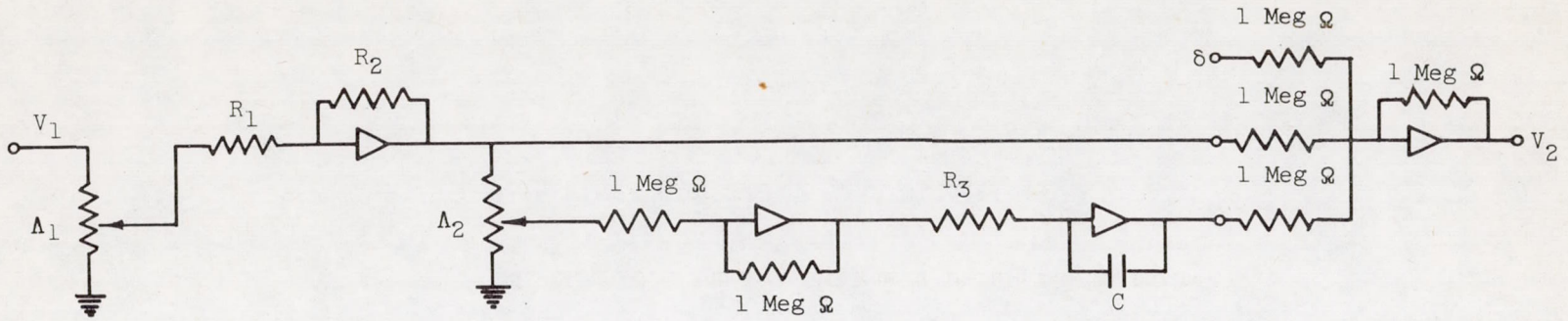

δ Disturbance function
▷ Operational amplifier

$$\frac{V_2}{V_1} = -K\left(1 + \frac{1}{\tau s}\right)$$

$$K = \Lambda_1 \frac{R_2}{R_1}$$

$$\tau = \frac{R_3 C}{\Lambda_2}$$

$$\frac{R_2}{R_1} = 10$$

$$R_3 = 0.1 \text{ Meg } \Omega$$

$$C = 0.1 \ \mu f$$

Λ = Percent of maximum potentiometer resistance/100

Figure 5. - Wiring diagram for proportional-plus-integral control.

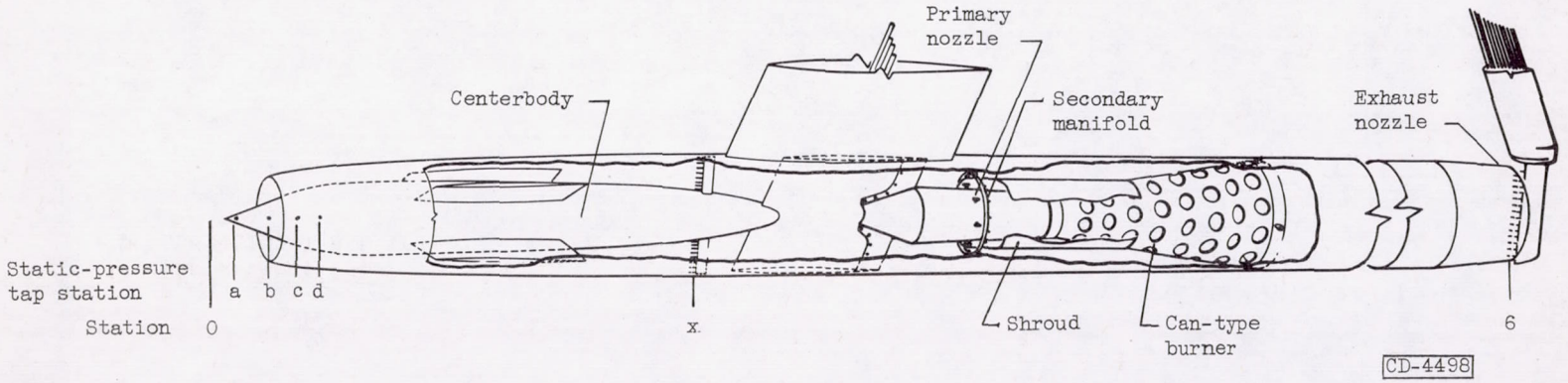

Figure 6. - Schematic diagram of 16-inch ram-jet engine.

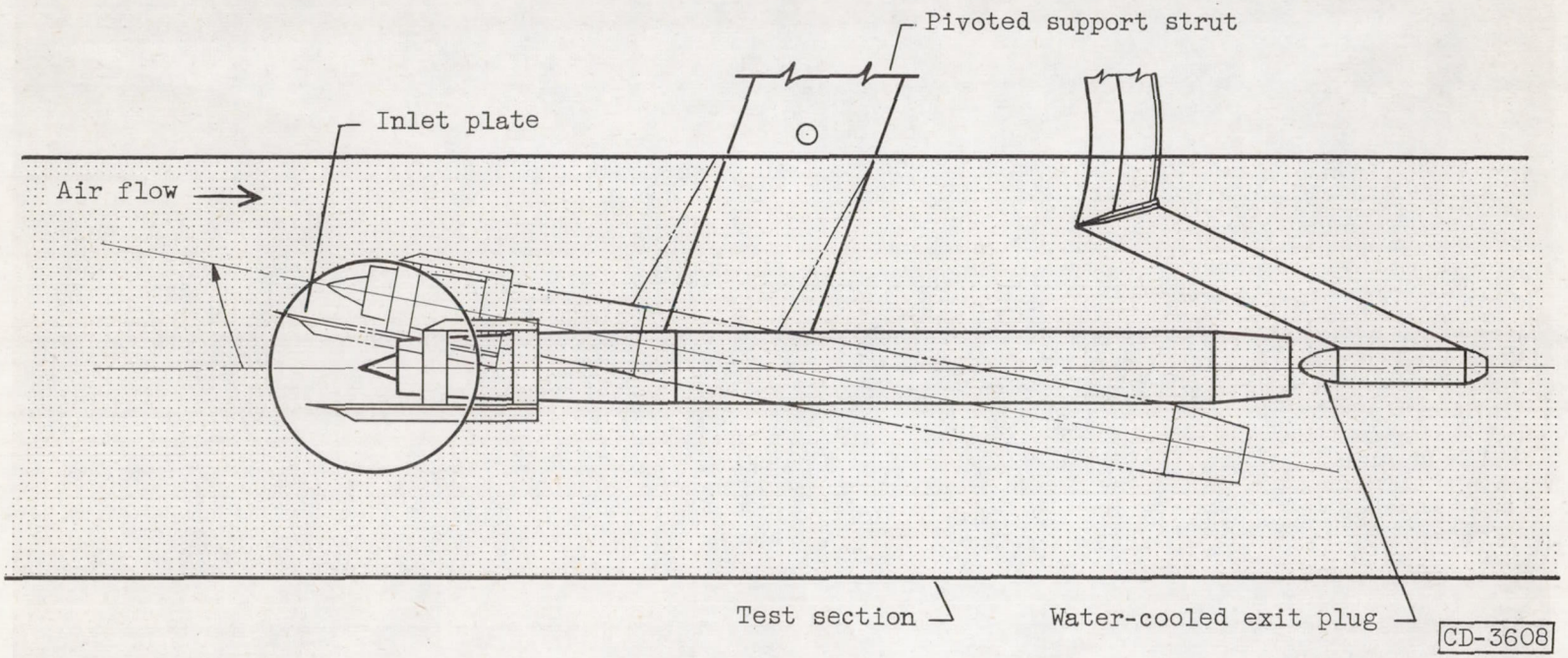

Figure 7. - Installation of 16-inch ram-jet engine in 8- by 6-foot supersonic wind tunnel.

Figure 8. - Sixteen-inch ram-jet engine with plate installed for disturbances in Mach number.

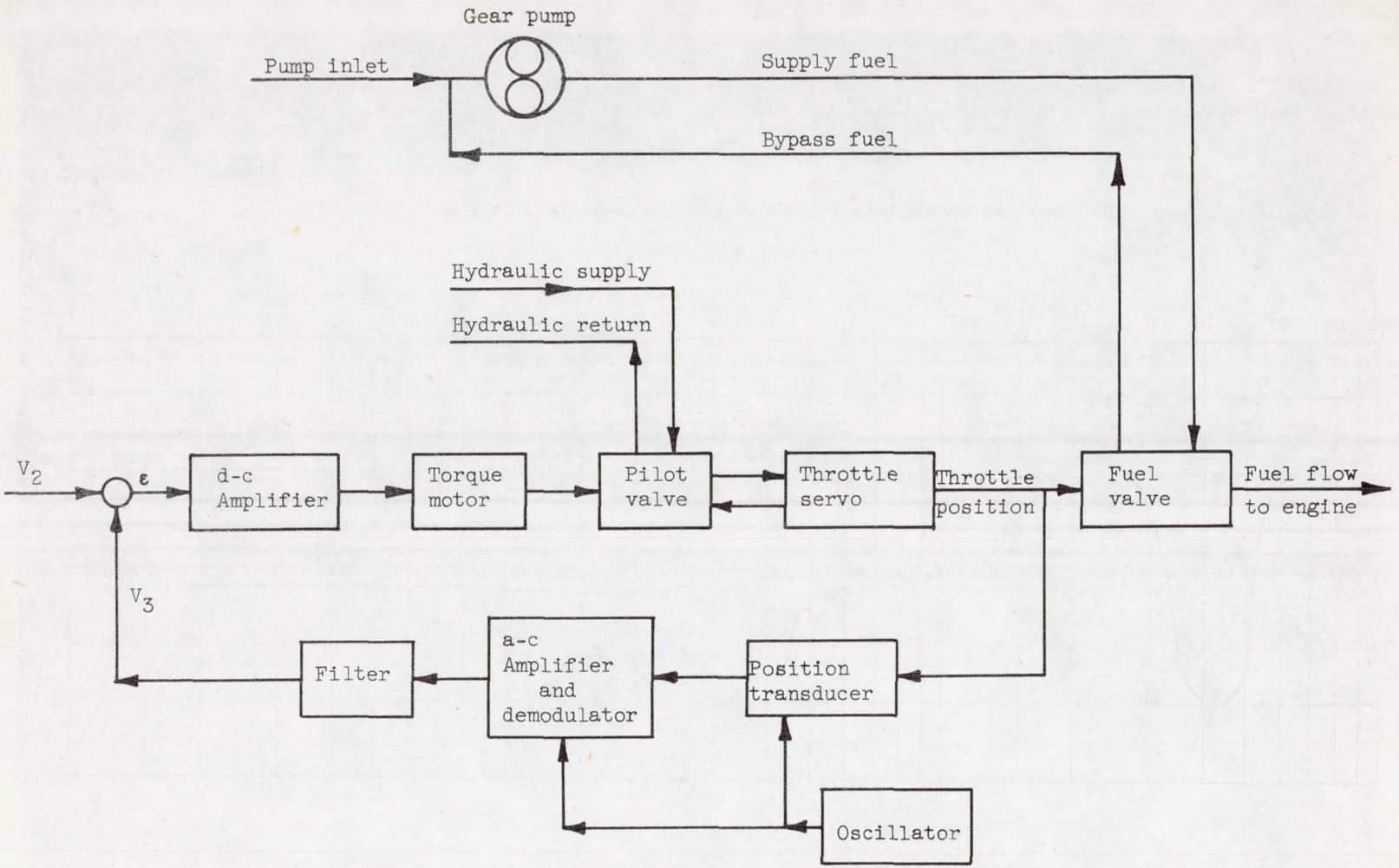

Figure 9. - Schematic diagram of control fuel system.

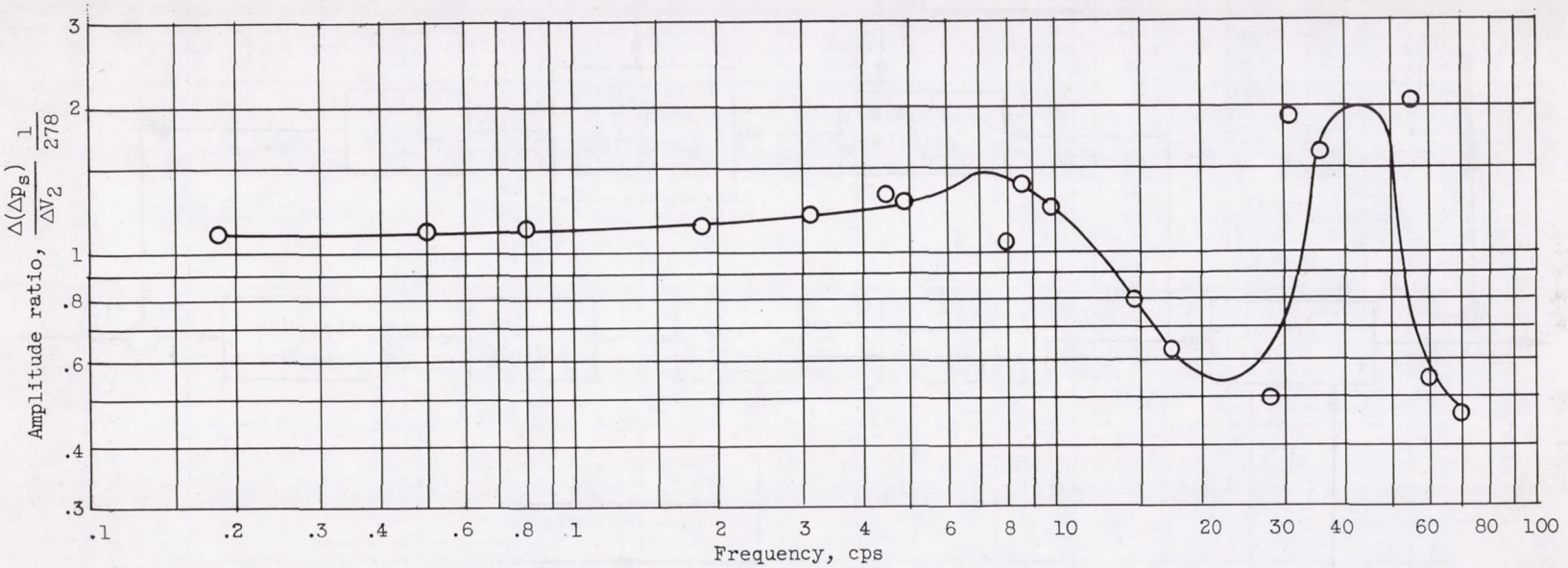

(a) Amplitude ratio.

Figure 10. - Typical frequency response of control fuel system as installed.

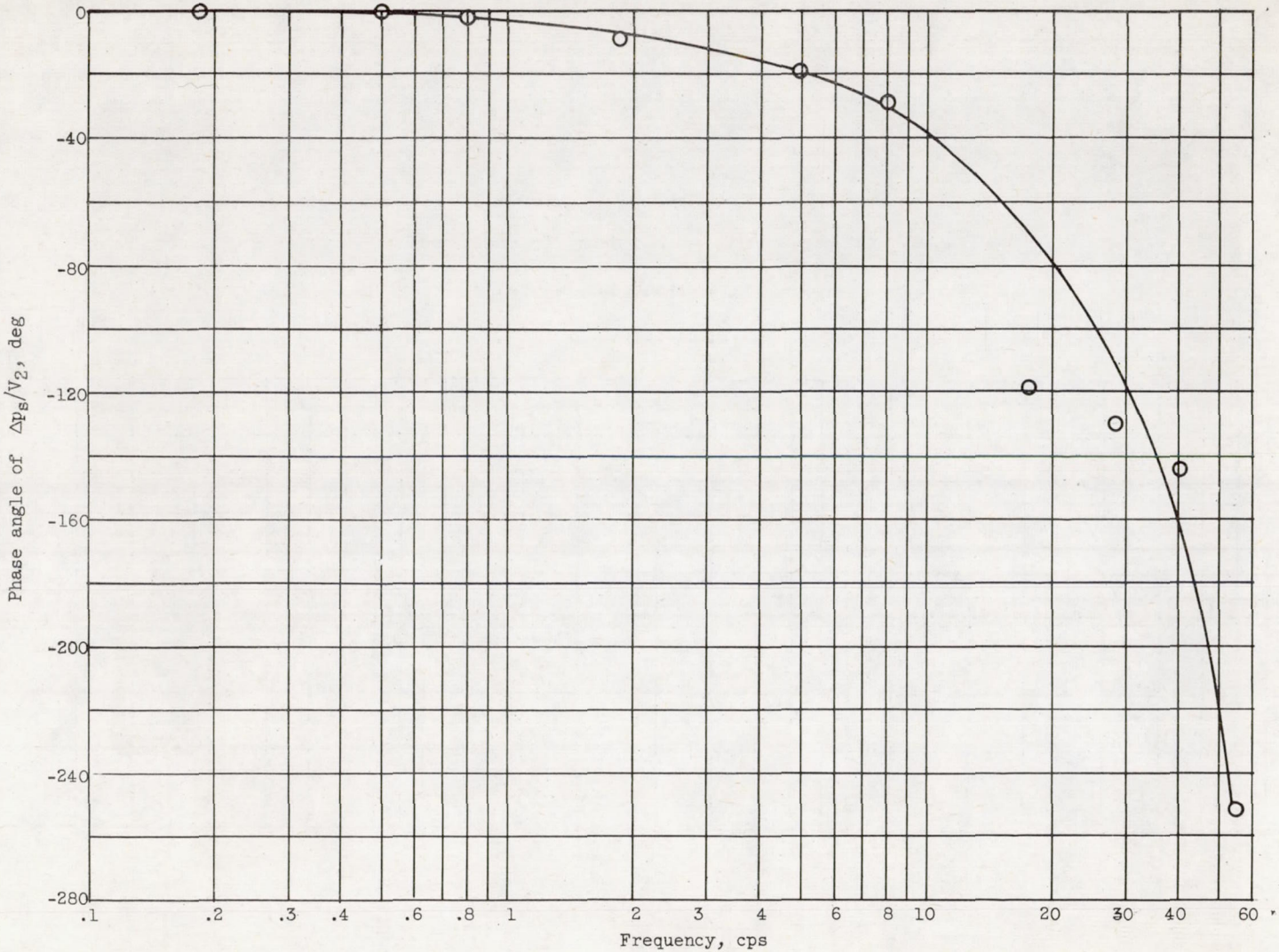

(b) Phase shift.

Figure 10. - Concluded. Typical frequency response of control fuel system as installed.

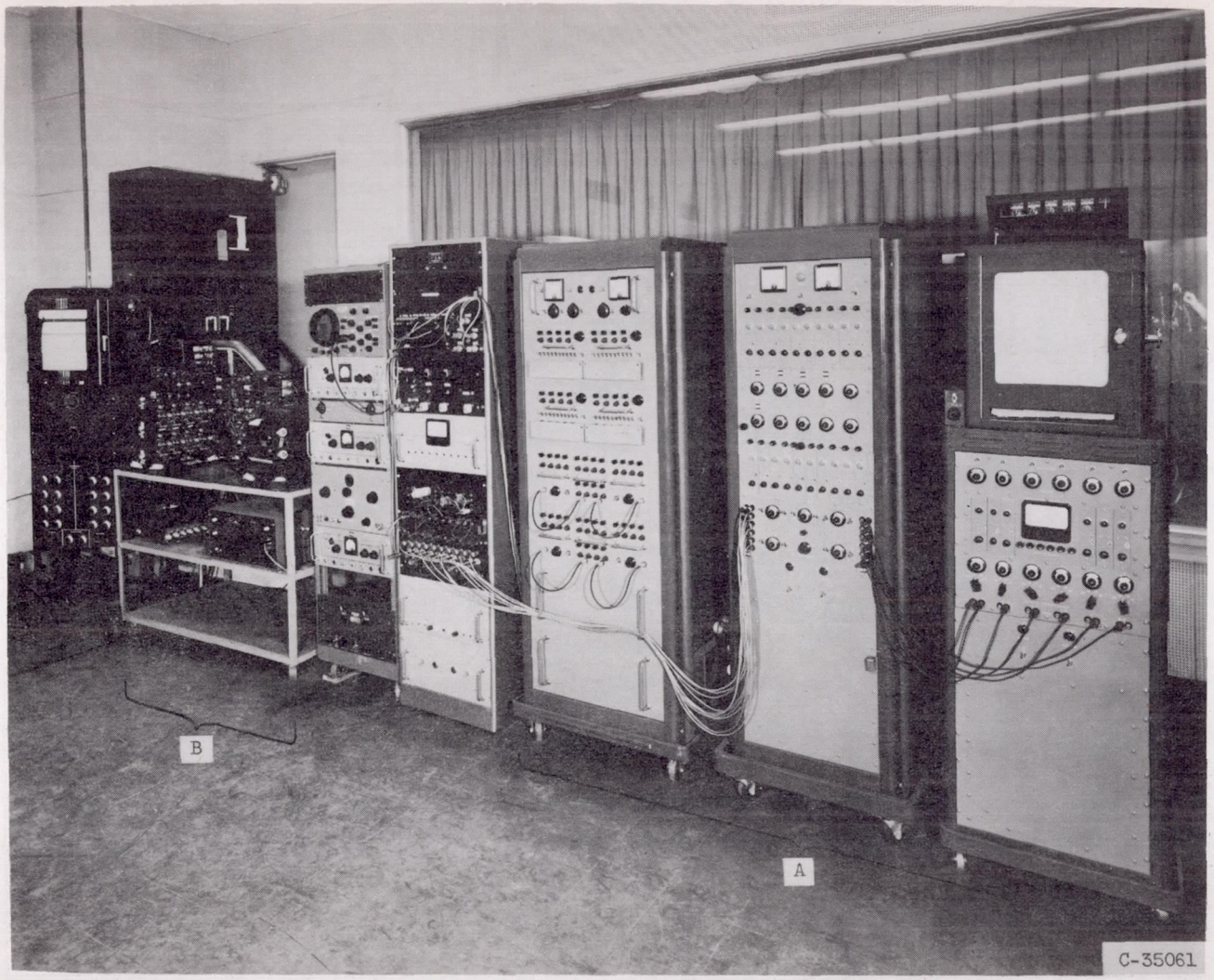

Figure 11. - Control equipment. A, electronic differential analyser and direct-inking recorder, B, carrier amplifiers and galvanometric oscillograph.

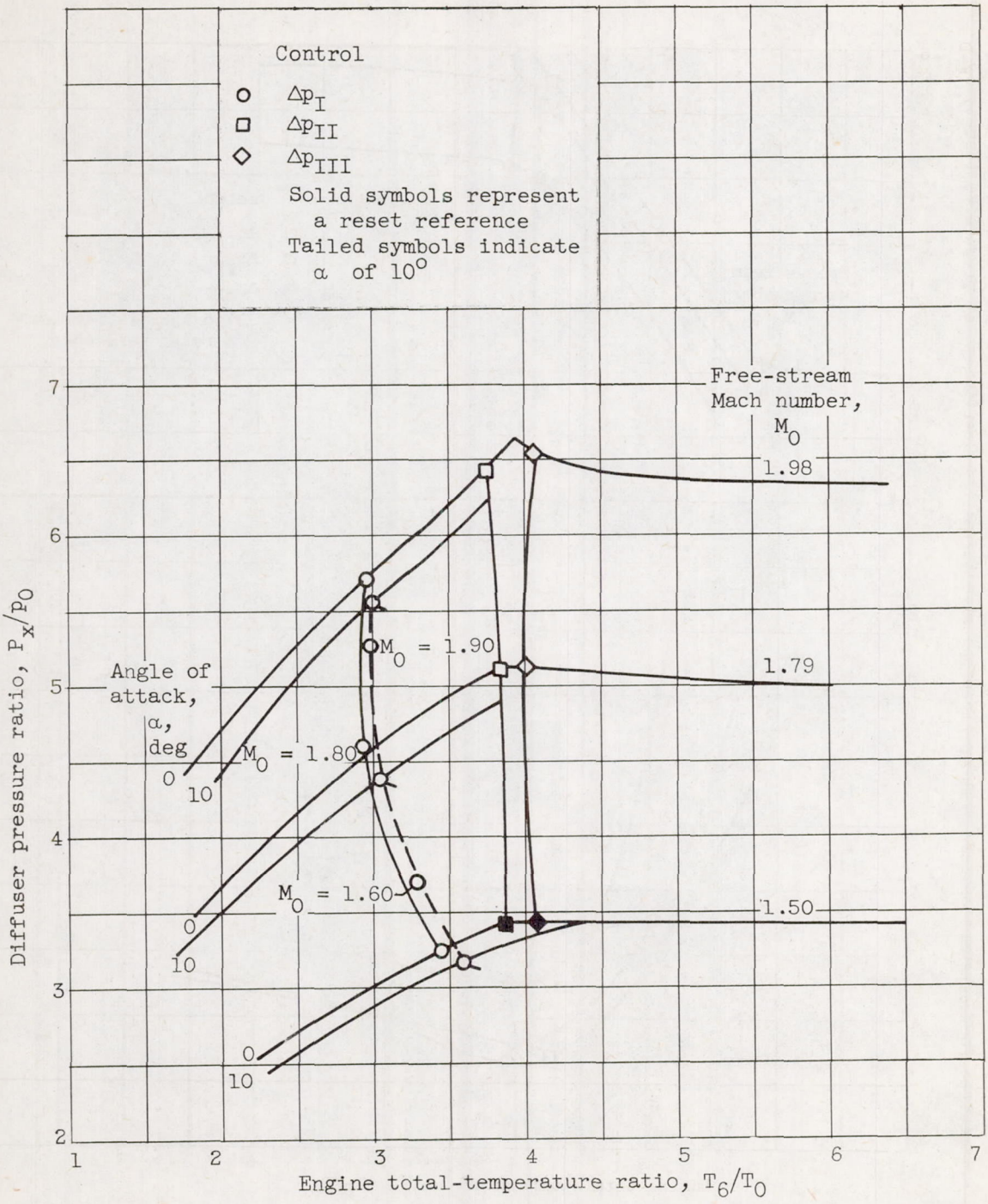

Figure 12. - Steady-state operation of controls in relation to diffuser performance.

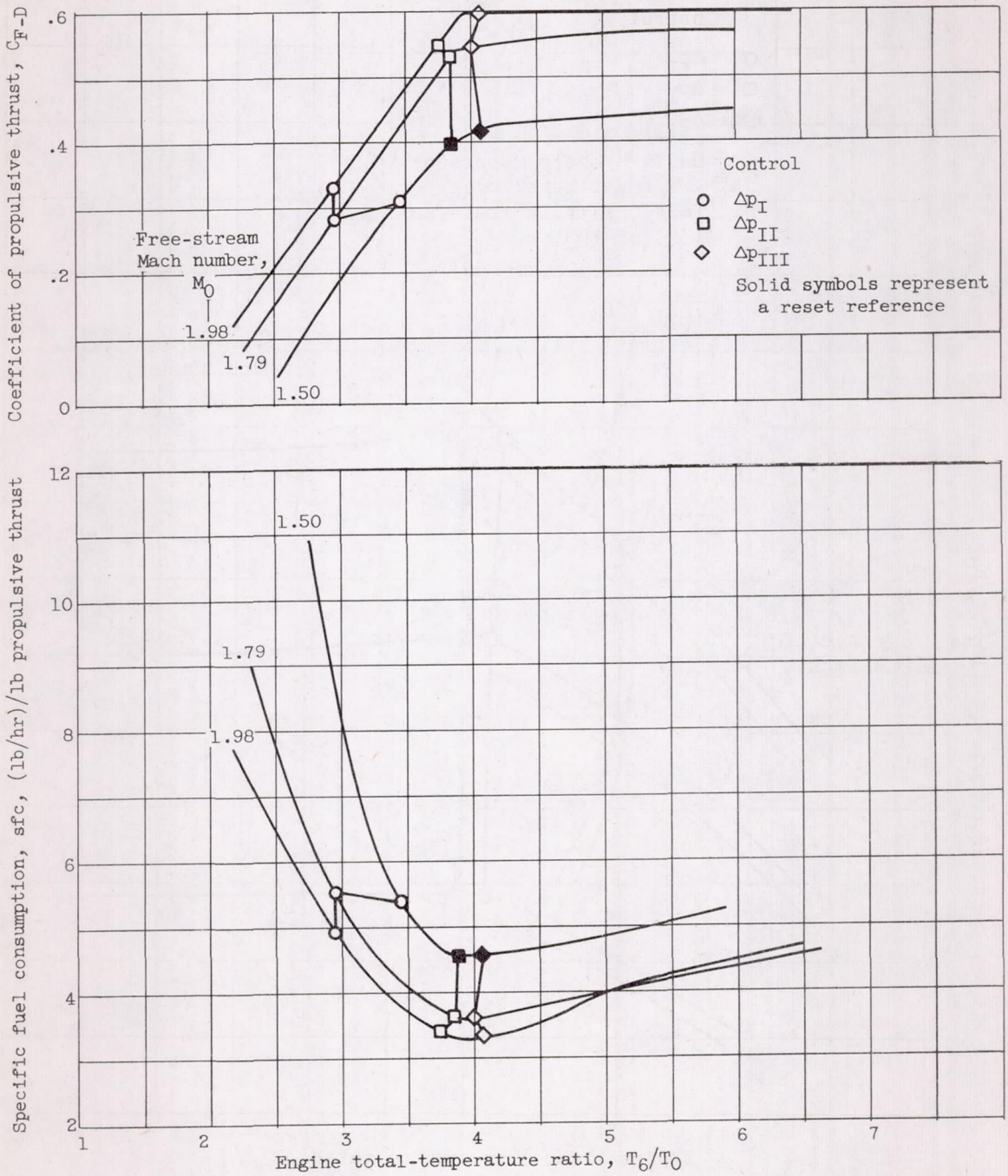

Figure 13. - Steady-state operation of controls in relation to engine performance. Zero angle of attack.

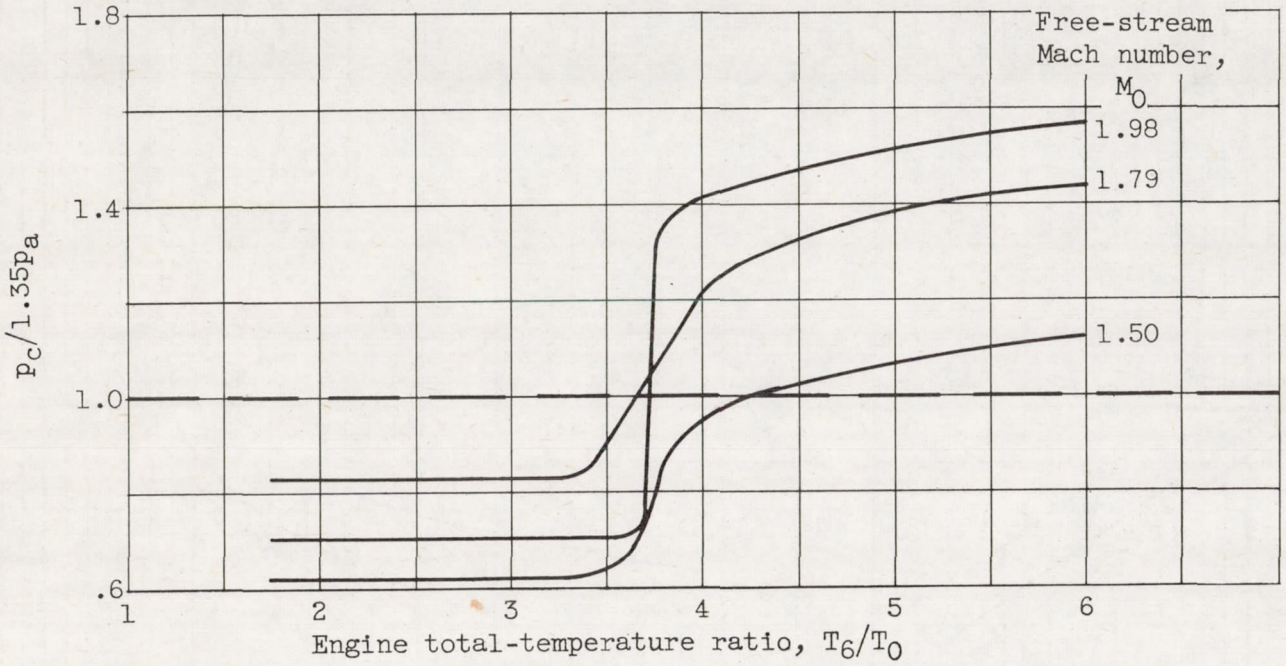

Figure 14. - Variation of ratio of controlled variable to reference setting with temperature ratio illustrating compensated reference technique. Zero angle of attack.

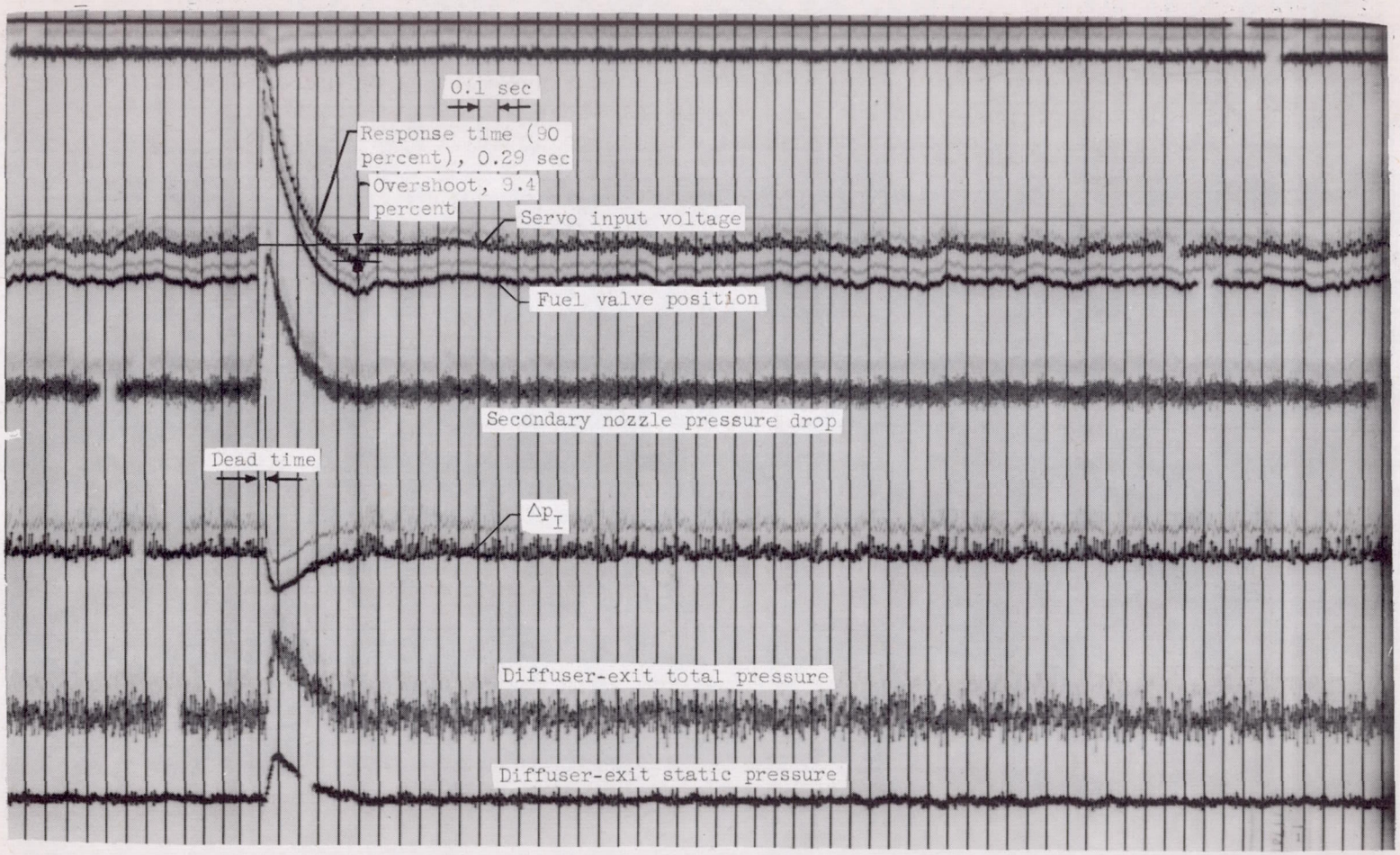

Figure 15. - Typical transient response of Δp_I control to fuel-flow disturbance. Fuel-flow disturbance, +556 pounds per hour; loop gain, 0.190; integrator time constant, 0.02 second; free-stream Mach number, 1.98; zero angle of attack.

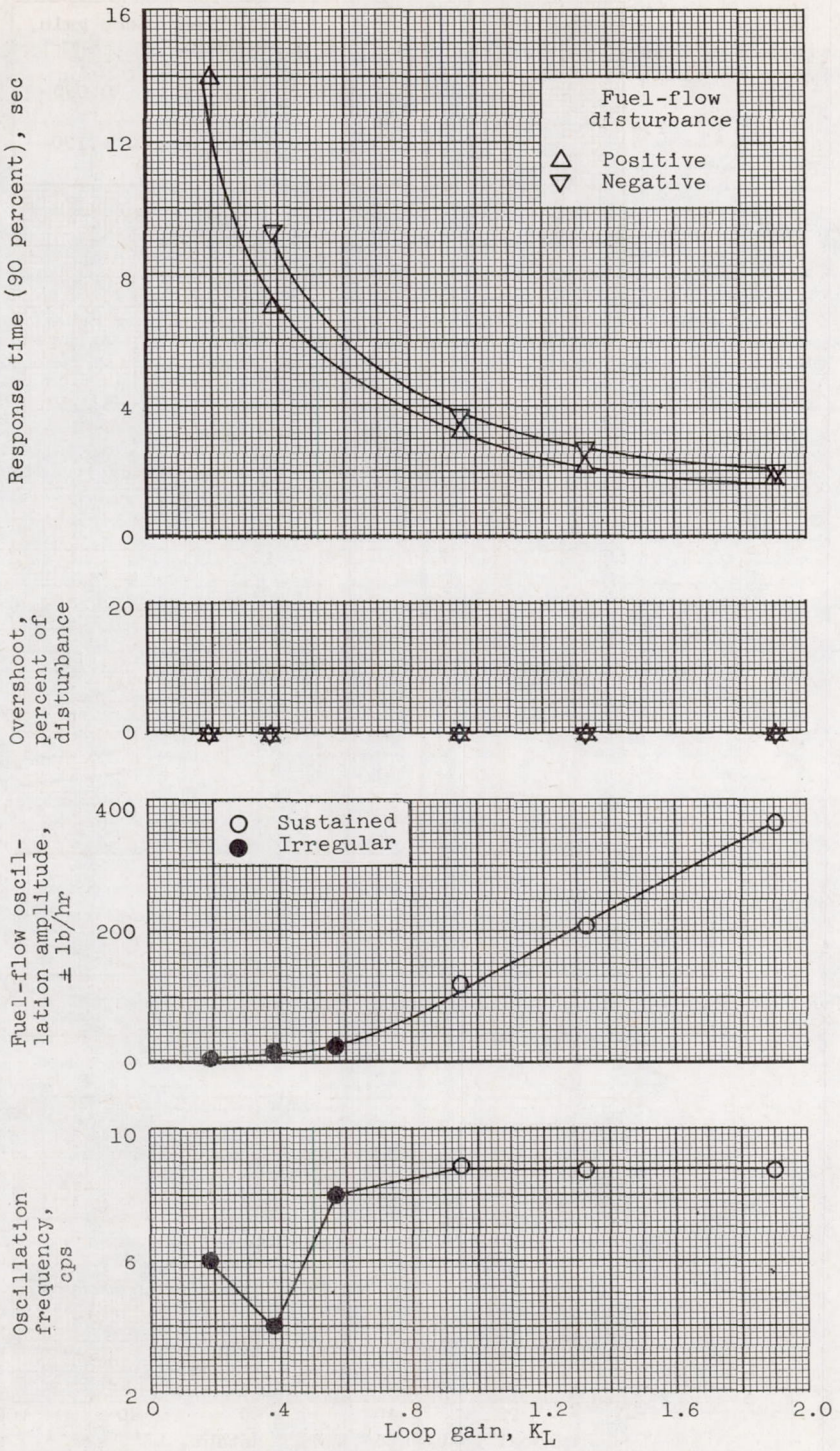

(a) Loop gain; reciprocal integrator time constant, 1.0 second^{-1}.

Figure 16. - Effect of loop gain and integrator time constant on response and stability of Δp_I control. Fuel-flow disturbance, ±556 pounds per hour; free-stream Mach number, 1.98; zero angle of attack.

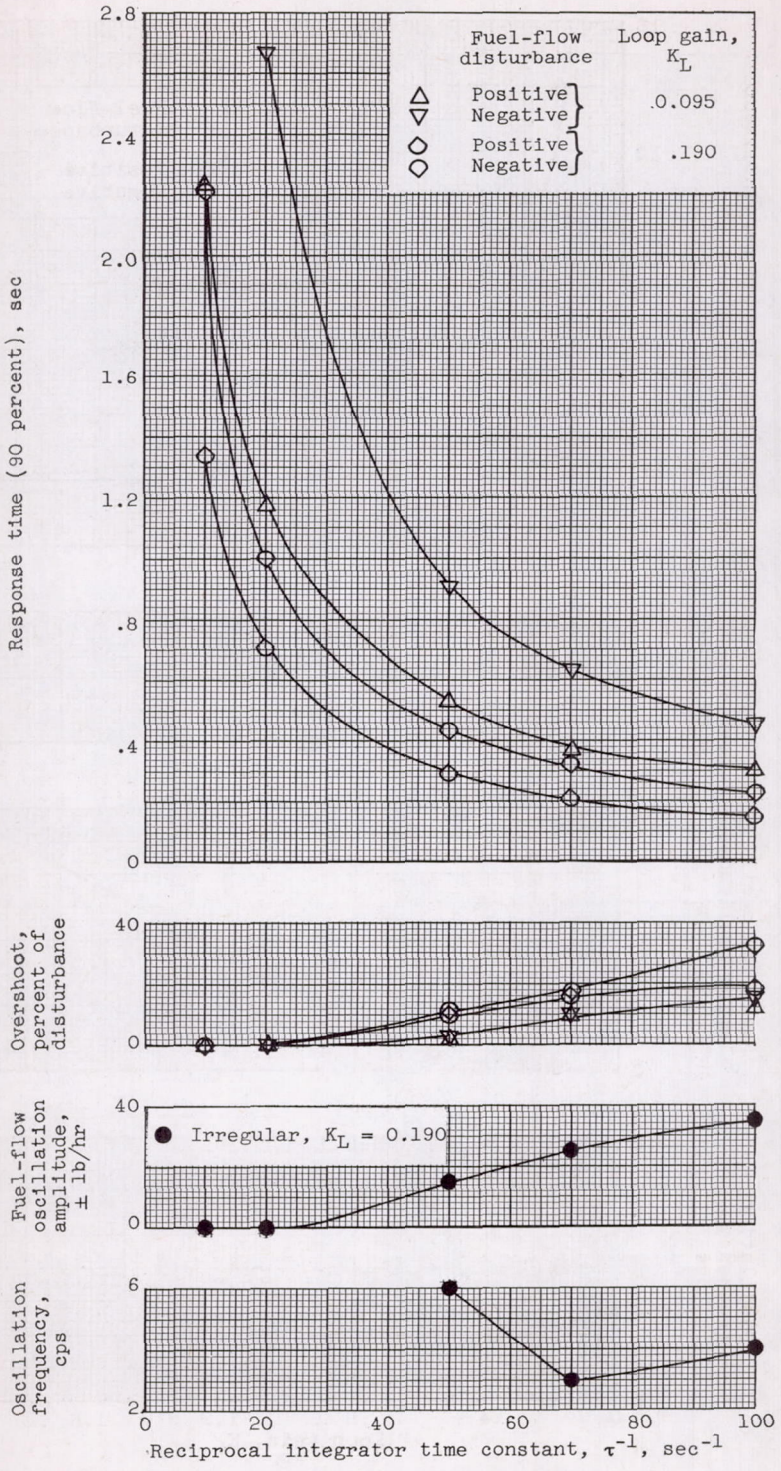

(b) Integrator time constant.

Figure 16. - Concluded. Effect of loop gain and integrator time constant on response and stability of Δp_I control. Fuel-flow disturbance, ±556 pounds per hour; free-stream Mach number, 1.98; zero angle of attack.

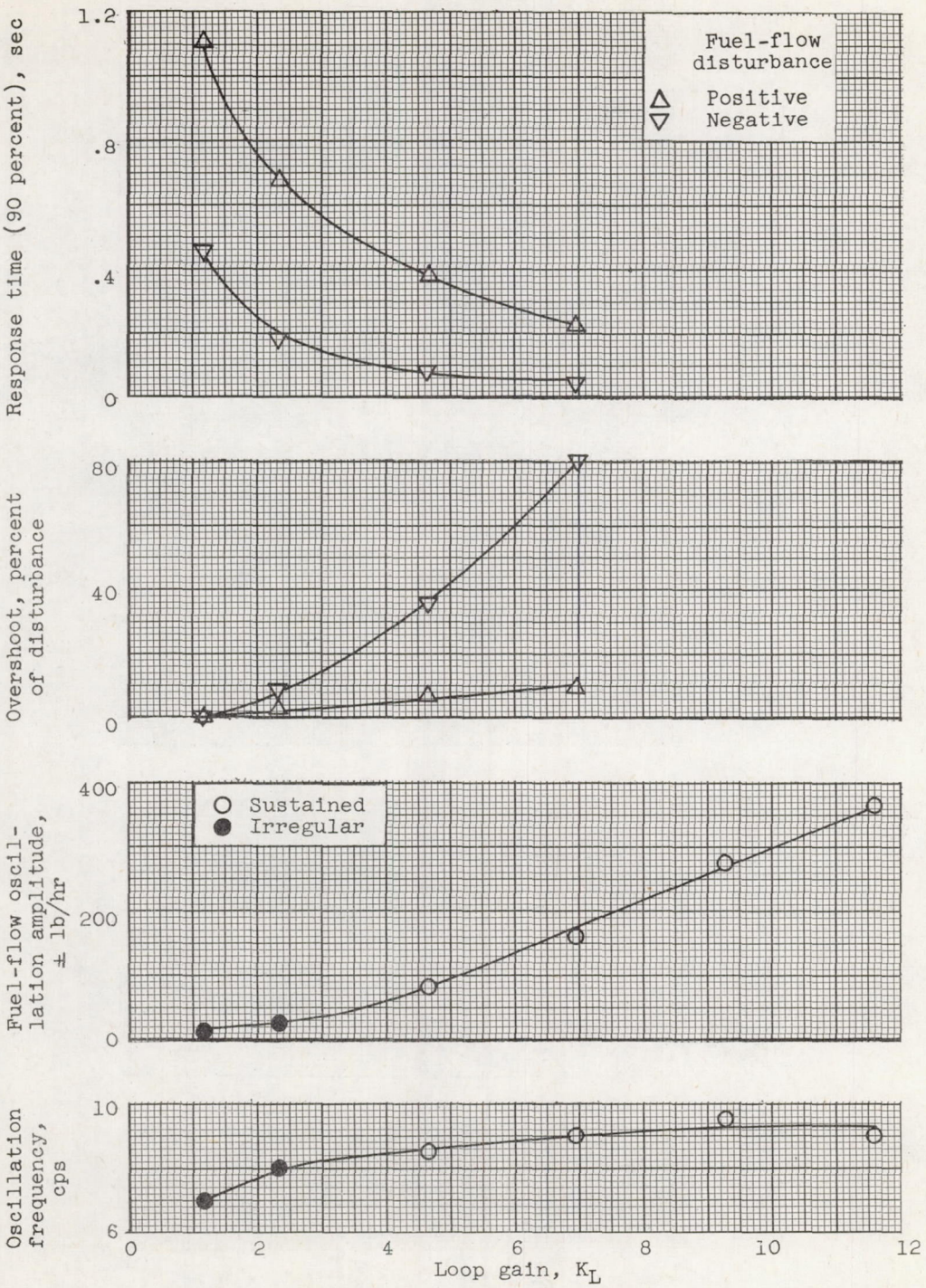

(a) Loop gain; reciprocal integrator time constant, 10 $second^{-1}$.

Figure 17. - Effect of loop gain and integrator time constant on response and stability of Δp_{II} control. Fuel-flow disturbance, ±278 pounds per hour; free-stream Mach number, 1.98; zero angle of attack.

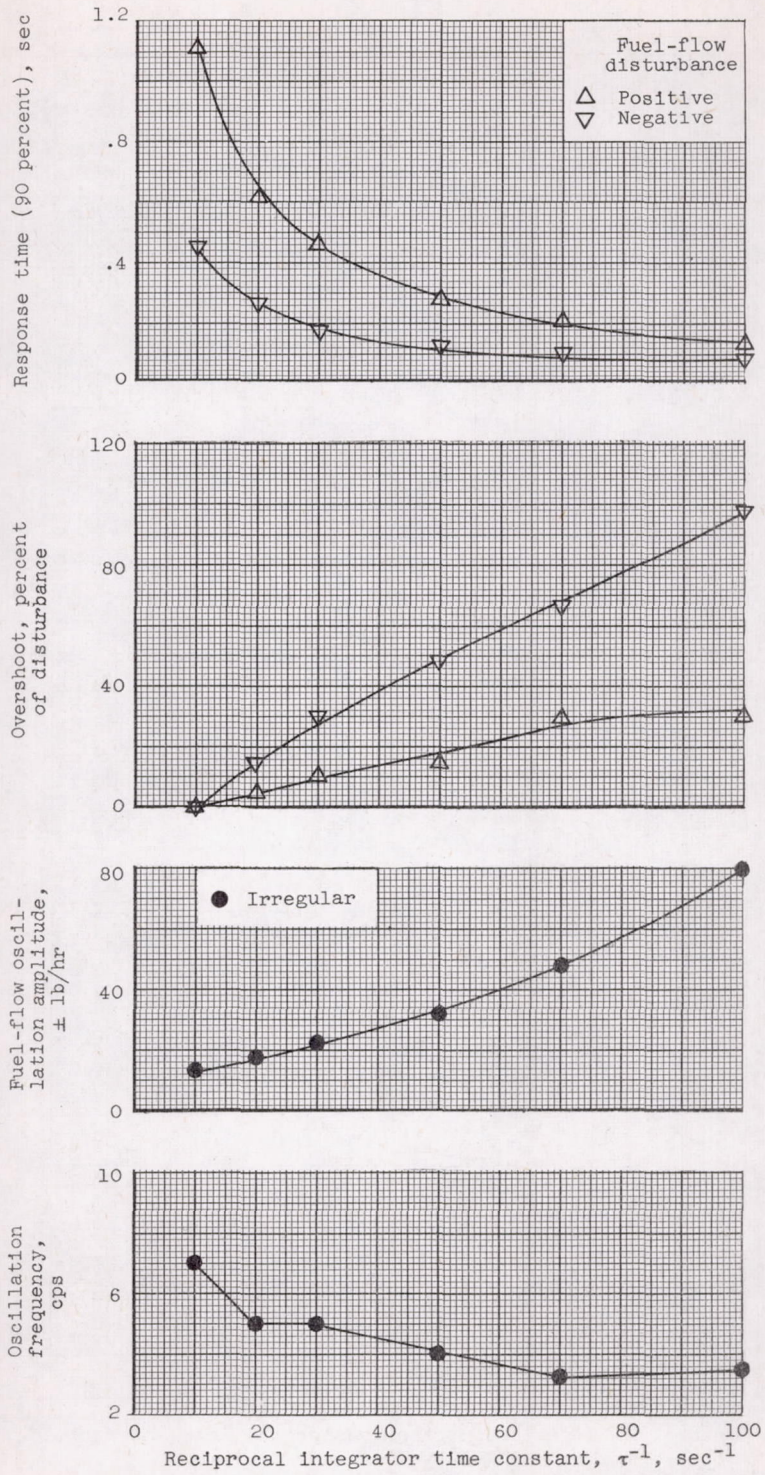

(b) Integrator time constant; loop gain, 1.16.

Figure 17. - Concluded. Effect of loop gain and integrator time constant on response and stability of ΔP_{II} control. Fuel-flow disturbance, ±278 pounds per hour; free-stream Mach number, 1.98; zero angle of attack.

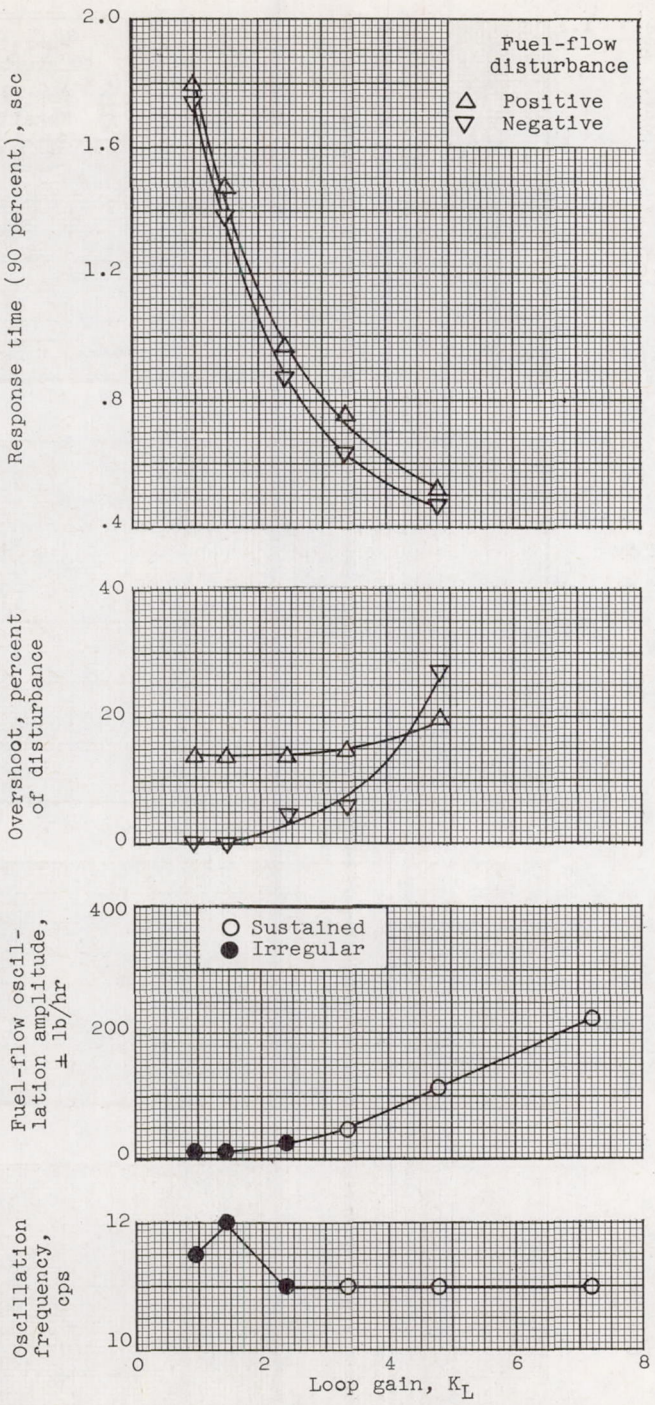

(a) Loop gain; reciprocal integrator time constant, 10 $second^{-1}$.

Figure 18. - Effect of loop gain and integrator time constant on response and stability of Δp_{III} control. Fuel-flow disturbance, ±278 pounds per hour; free-stream Mach number, 1.98; zero angle of attack.

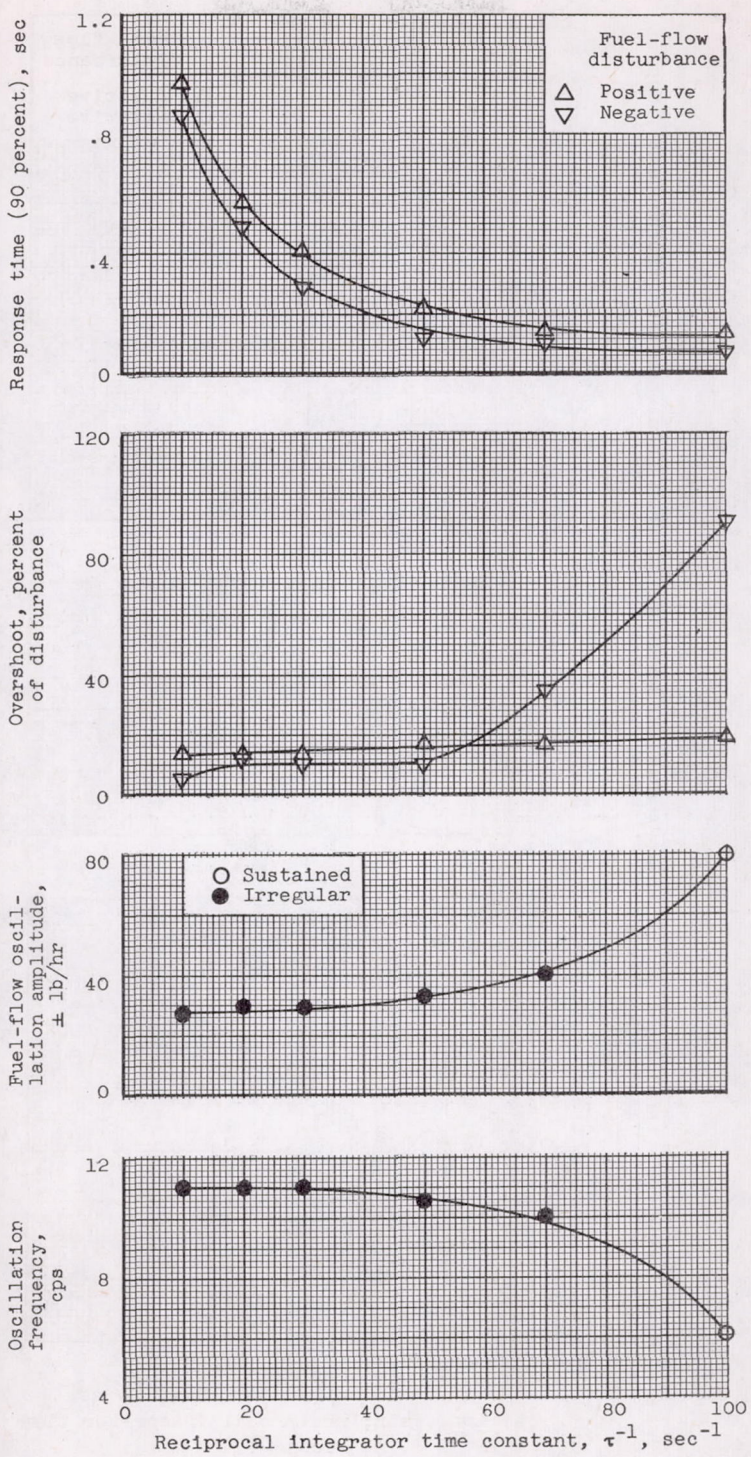

(b) Integrator time constant; loop gain, 2.40.

Figure 18. - Concluded. Effect of loop gain and integrator time constant on response and stability of Δp_{III} control. Fuel-flow disturbance, ±278 pounds per hour; free-stream Mach number, 1.98; zero angle of attack.

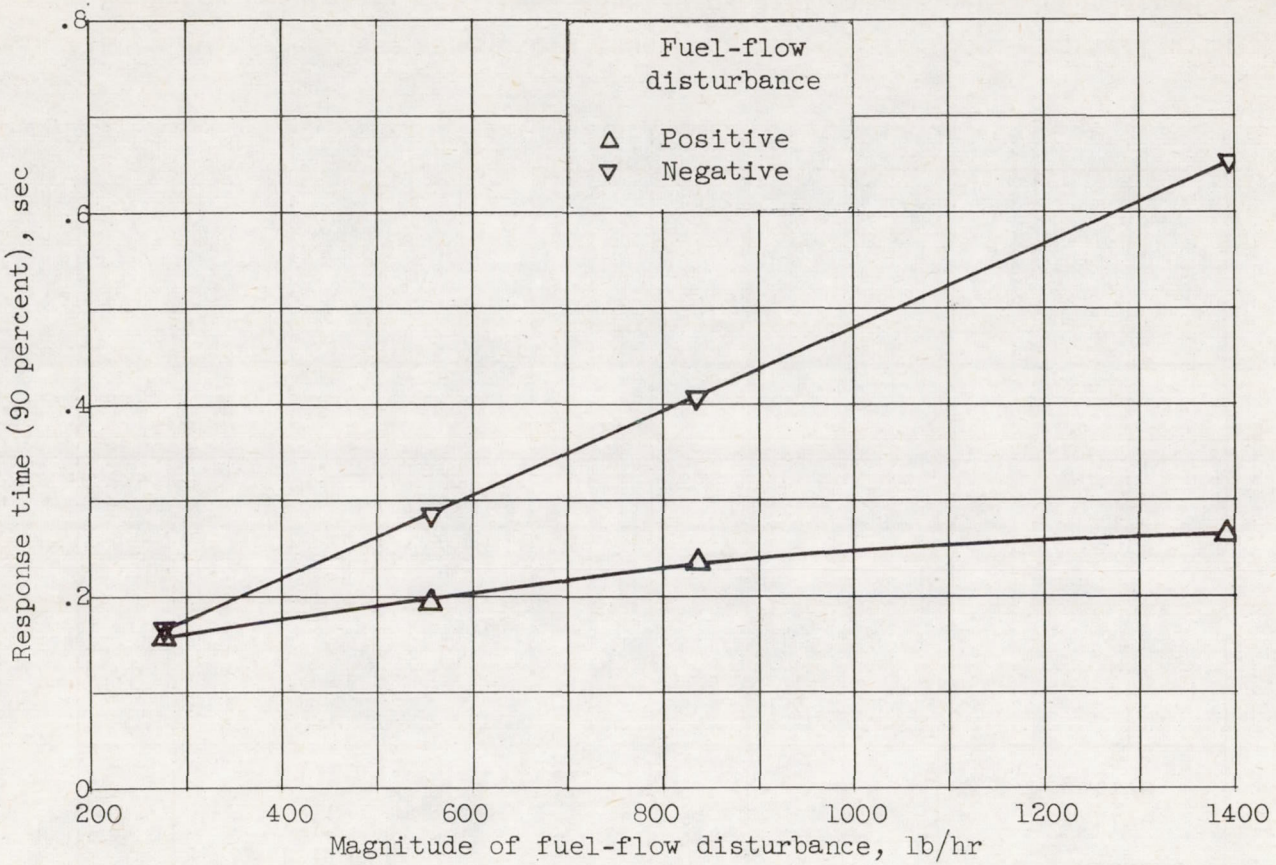

Figure 19. - Effect of magnitude of fuel-flow disturbance on response time of Δp_I control. Loop gain, 0.286; integrator time constant, 0.02 second; free-stream Mach number, 1.98; zero angle of attack.

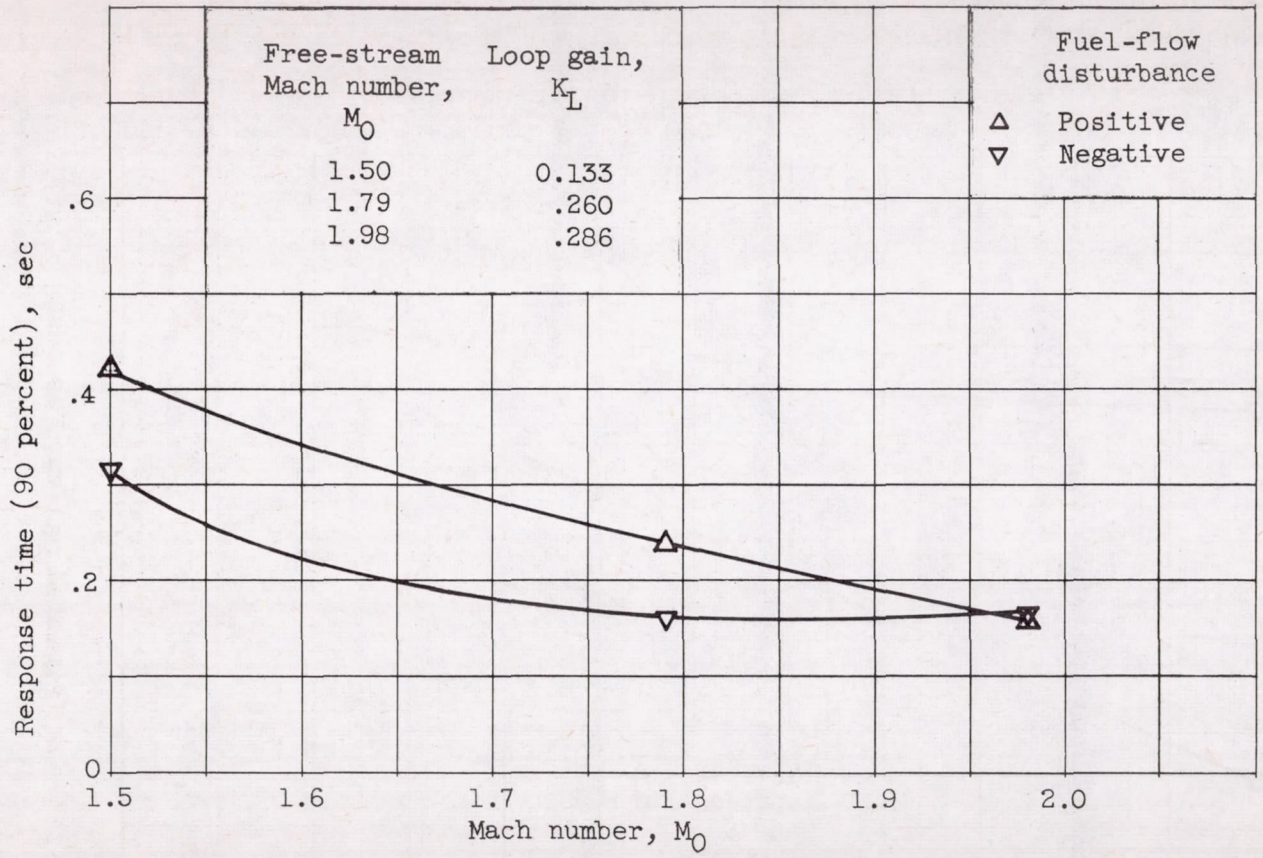

Figure 20. - Response time at various Mach numbers for Δp_I control with constant controller settings. Fuel-flow disturbance, ±278 pounds per hour; integrator time constant, 0.02 second; zero angle of attack.

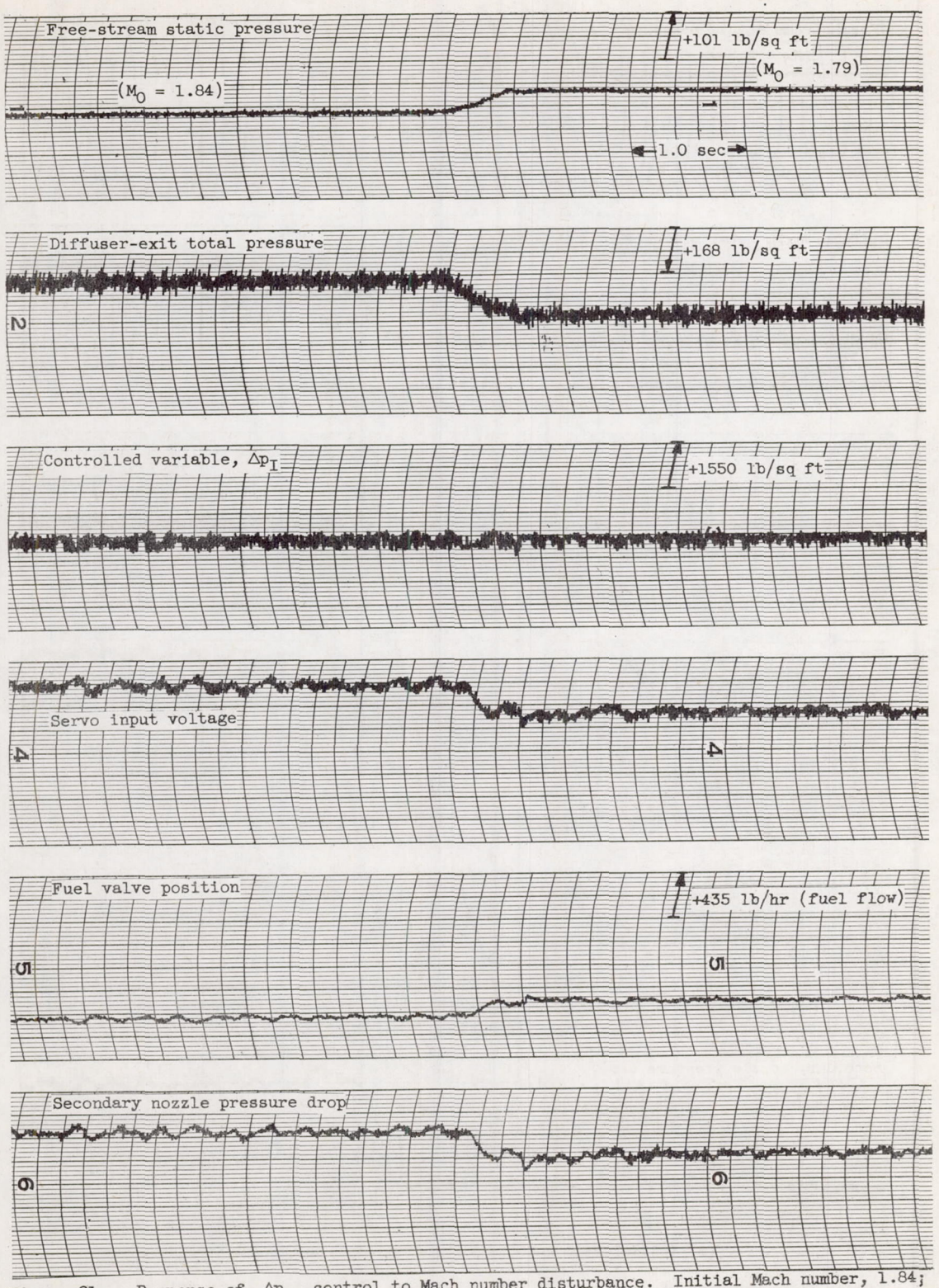

Figure 21. - Response of Δp_I control to Mach number disturbance. Initial Mach number, 1.84; final Mach number, 1.79; loop gain at free-stream Mach number of 1.79, 0.262; integrator time constant, 0.02 second; zero angle of attack.

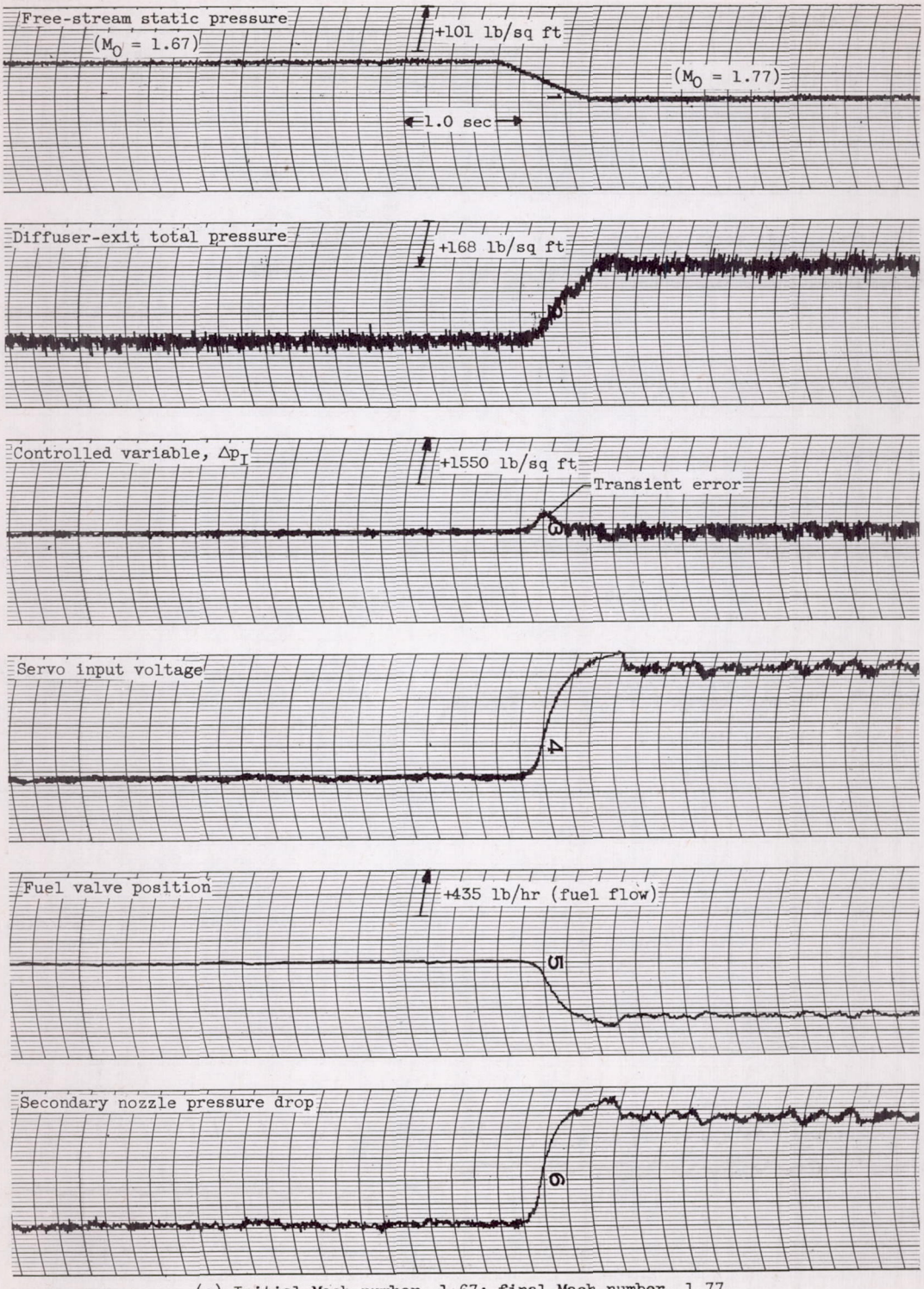

(a) Initial Mach number, 1.67; final Mach number, 1.77.

Figure 22. - Response of Δp_I control to Mach number disturbance. Loop gain at free-stream Mach number of 1.79, 0.262; integrator time constant, 0.02 second; zero angle of attack.

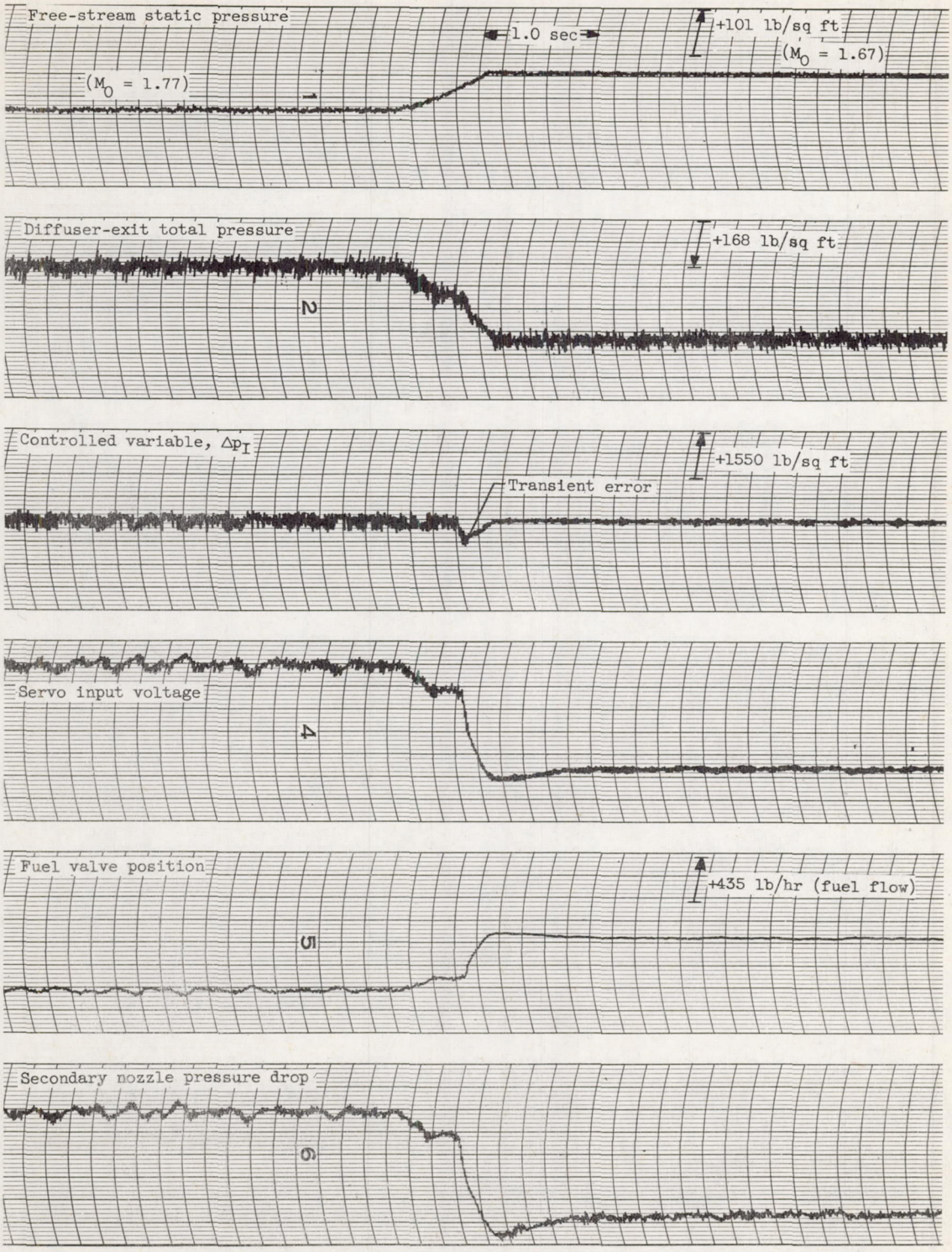

(b) Initial Mach number, 1.77; final Mach number, 1.67.

Figure 22. - Concluded. Response of Δp_I control to Mach number disturbance. Loop gain at free-stream Mach number of 1.79, 0.262; integrator time constant, 0.02 second; zero angle of attack.

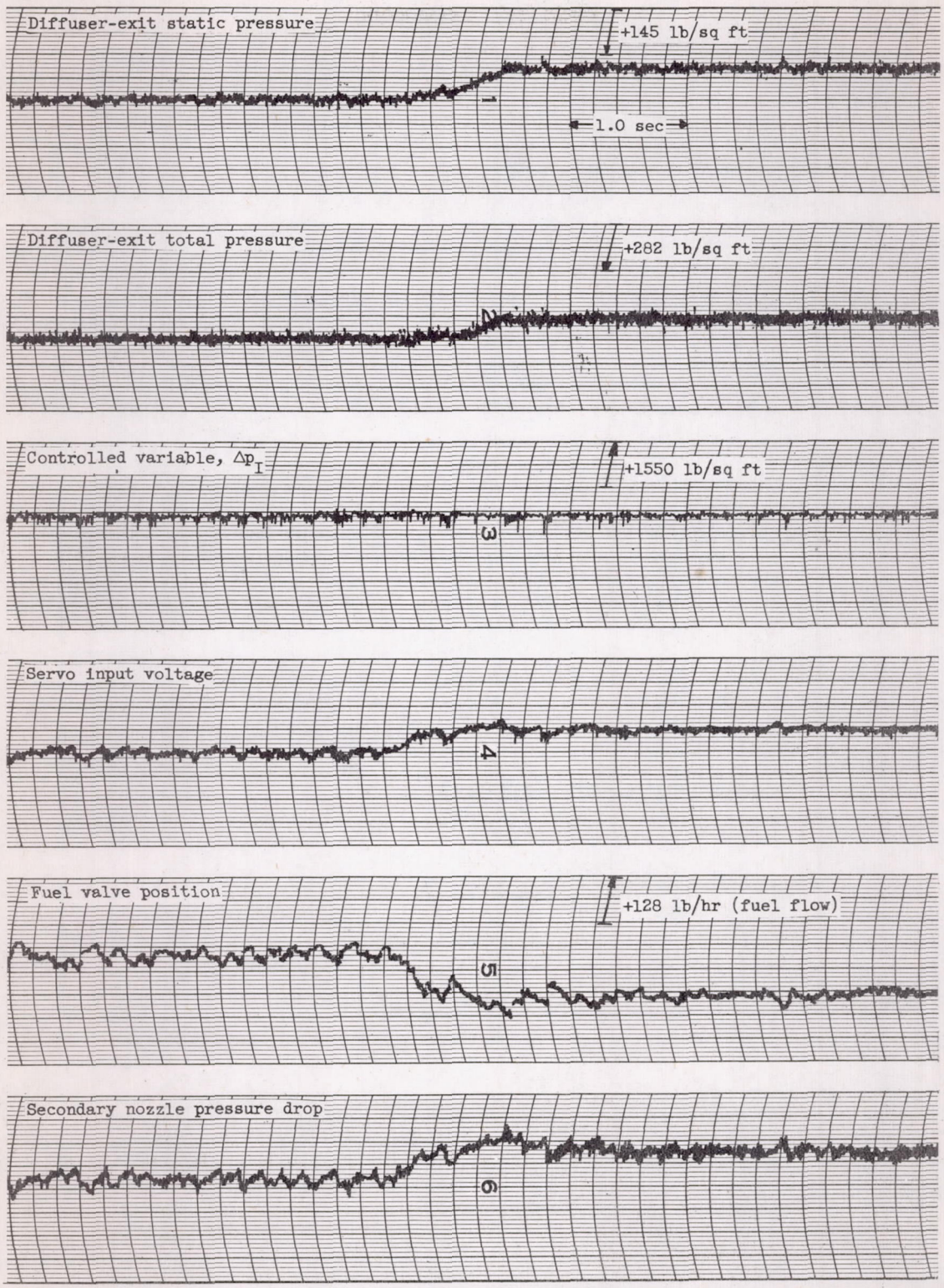

Figure 23. - Response of Δp_I control to angle-of-attack disturbance. Initial angle of attack, 0°; final angle of attack, 10°; loop gain at zero angle of attack, 0.286; integrator time constant, 0.02 second; free-stream Mach number, 1.98.

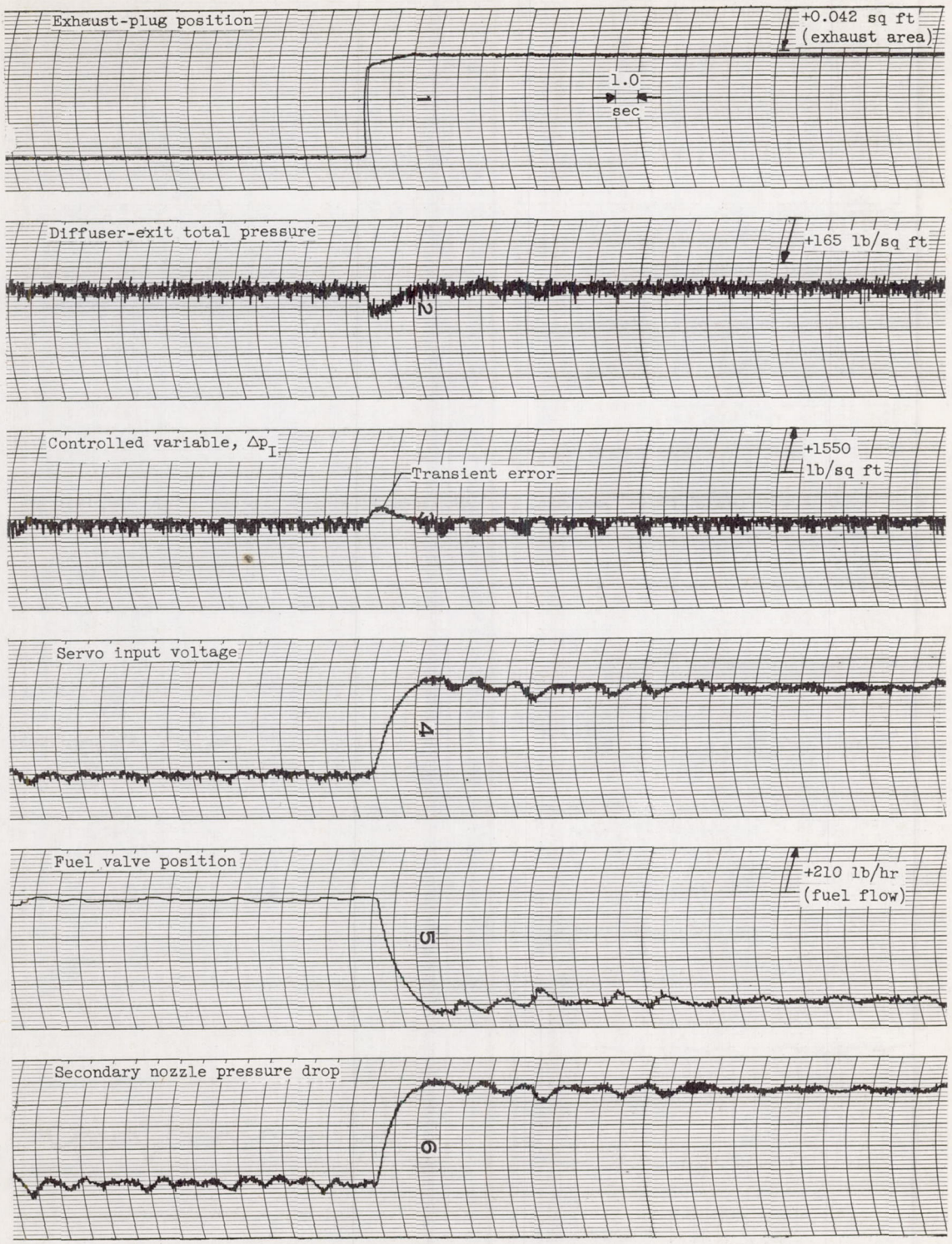

(a) Initial exhaust area, 0.960 square foot; final exhaust area, 0.864 square foot.

Figure 24. - Response of Δp_I control to exhaust-area disturbance. Loop gain at exhaust area of 0.960 square foot, 0.262; integrator time constant, 0.02 second; free-stream Mach number, 1.77; zero angle of attack.

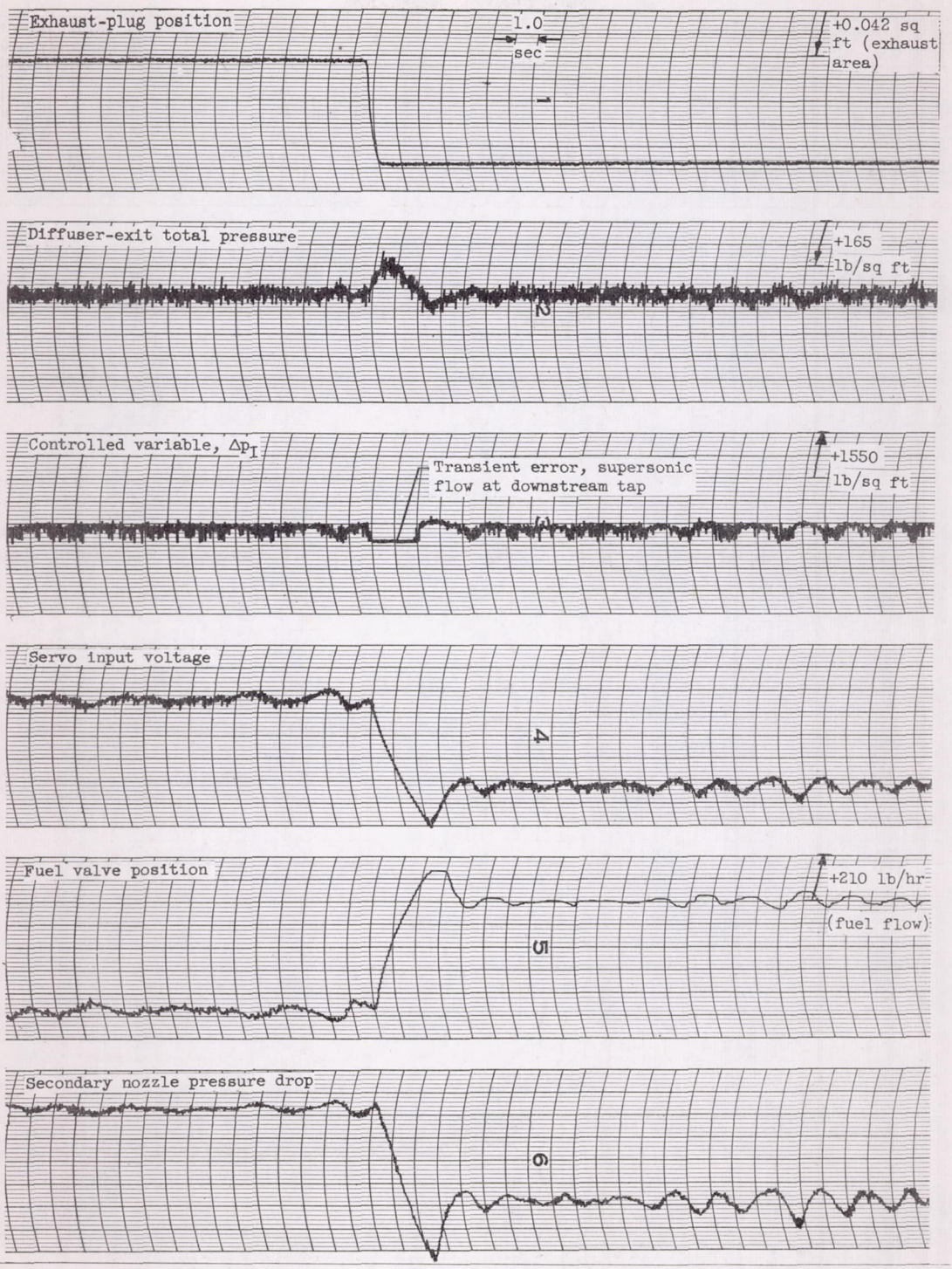

(b) Initial exhaust area, 0.864 square foot; final exhaust area, 0.960 square foot.

Figure 24. - Concluded. Response of Δp_I control to exhaust-area disturbance. Loop gain at exhaust area of 0.960 square foot, 0.262; integrator time constant, 0.02 second; free-stream Mach number, 1.77; zero angle of attack.

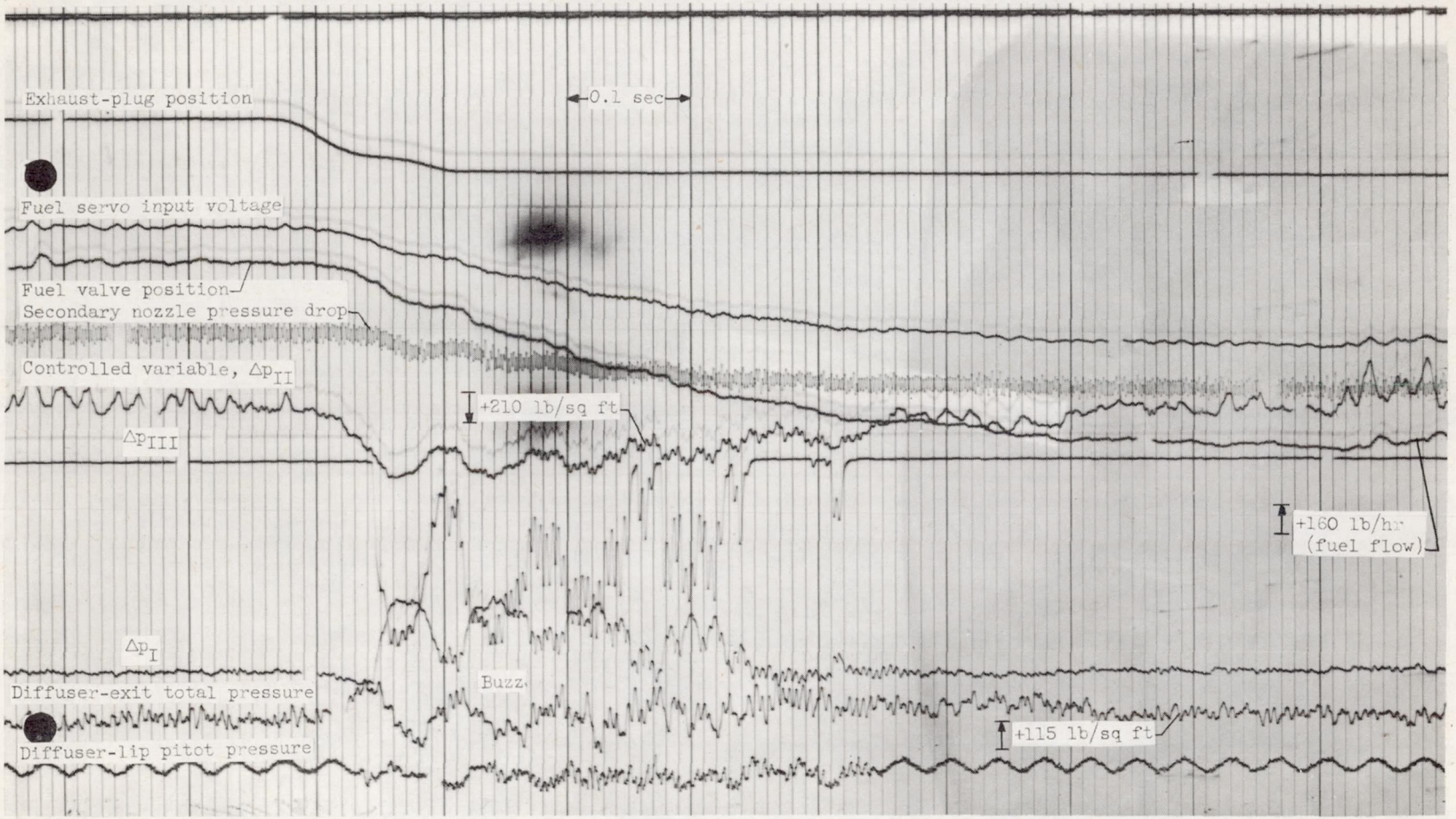

(a) Initial exhaust area, 0.960 square foot; final exhaust area, 0.755 square foot.

Figure 25. - Response of Δp_{II} control to exhaust-area disturbance. Loop gain at exhaust area of 0.960 square foot, 2.32; integrator time constant, 0.033 second; free-stream Mach number, 1.98; zero angle of attack.

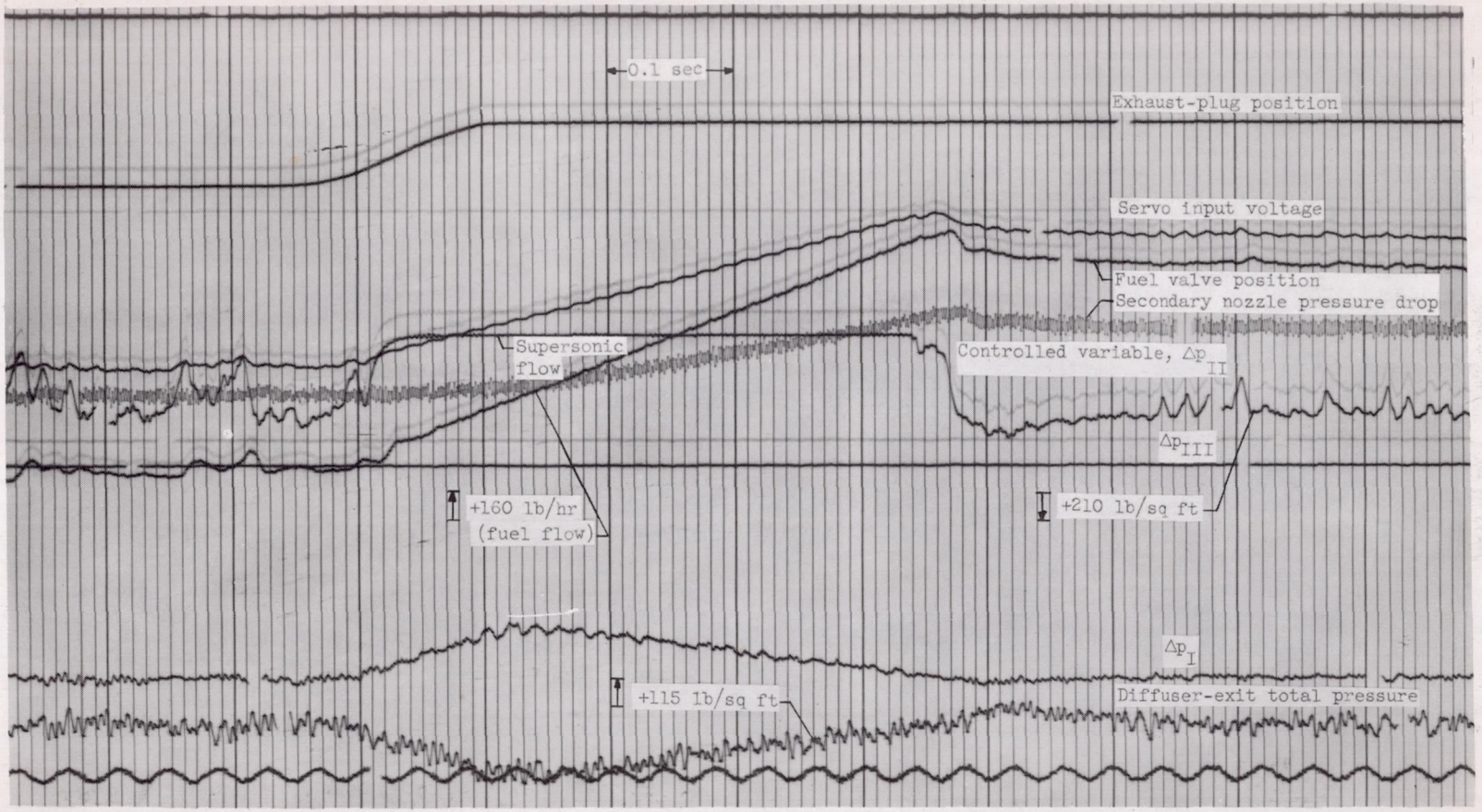

(b) Initial exhaust area, 0.755 square foot; final exhaust area, 0.960 square foot.

Figure 25. - Concluded. Response of Δp_{II} control to exhaust-area disturbance. Loop gain at exhaust area of 0.960 square foot, 2.32; integrator time constant, 0.033 second; free-stream Mach number, 1.98; zero angle of attack.

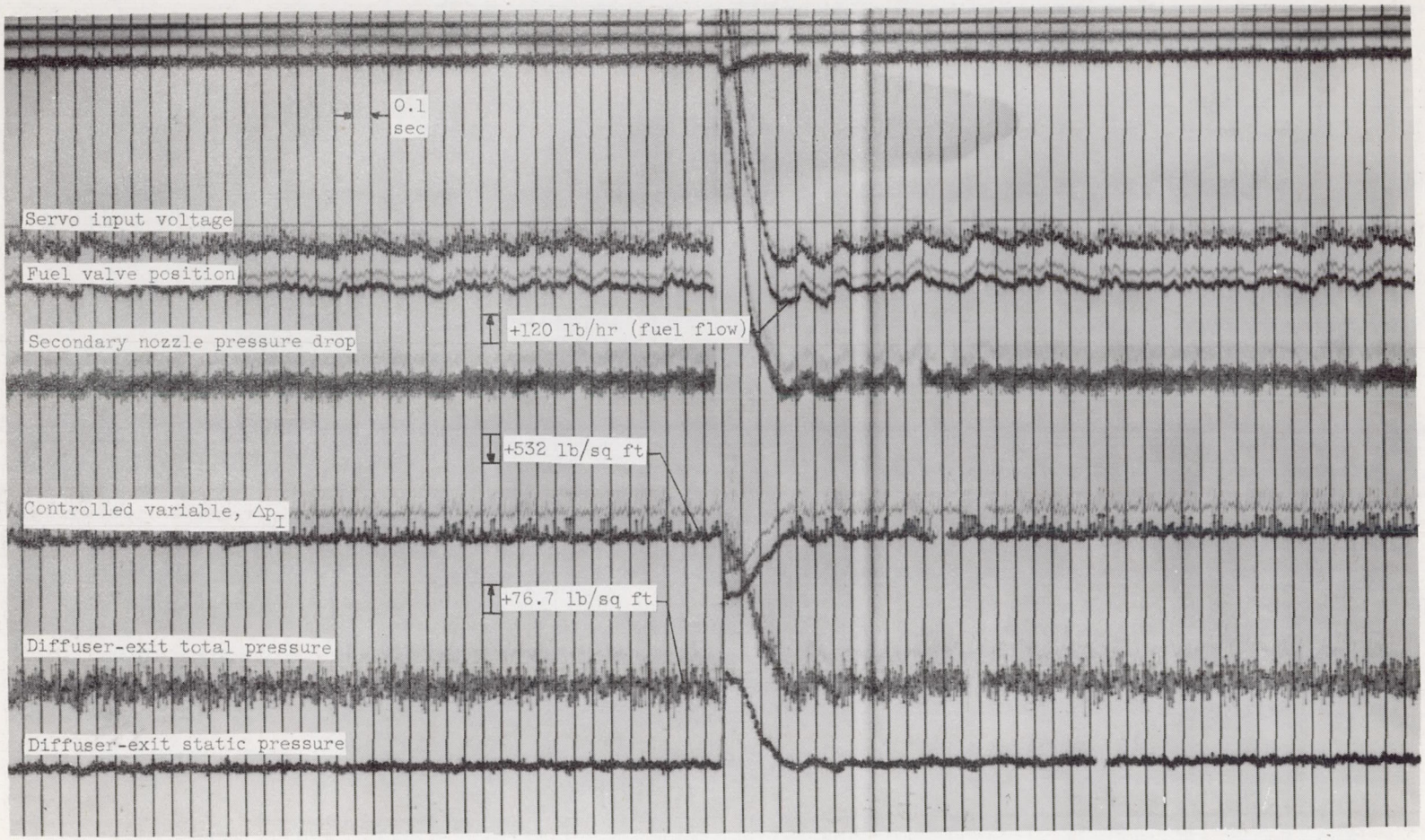

(a) Control, Δp_I; fuel-flow disturbance, +1390 pounds per hour; loop gain, 0.286; integrator time constant, 0.02 second.

Figure 26. - Transient response of controls to disturbance into subcritical. Free-stream Mach number, 1.98; zero angle of attack.

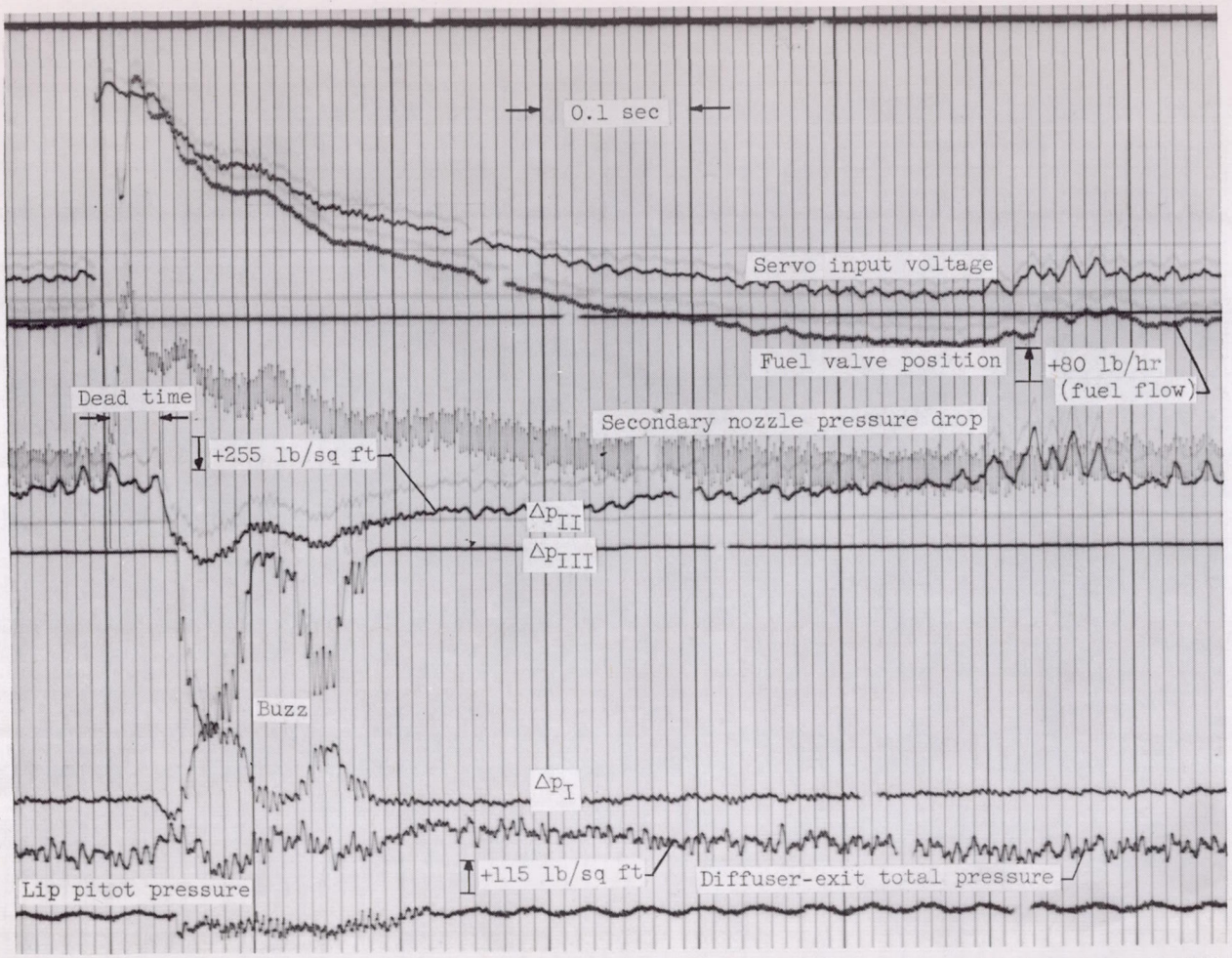

b) Control, Δp_{II}; fuel-flow disturbance, +556 pounds per hour; loop gain, 2.32; integrator time constant, 0.033 second.

Figure 26. - Continued. Transient response of controls to disturbance into subcritical. Free-stream Mach number, 1.98; zero angle of attack.

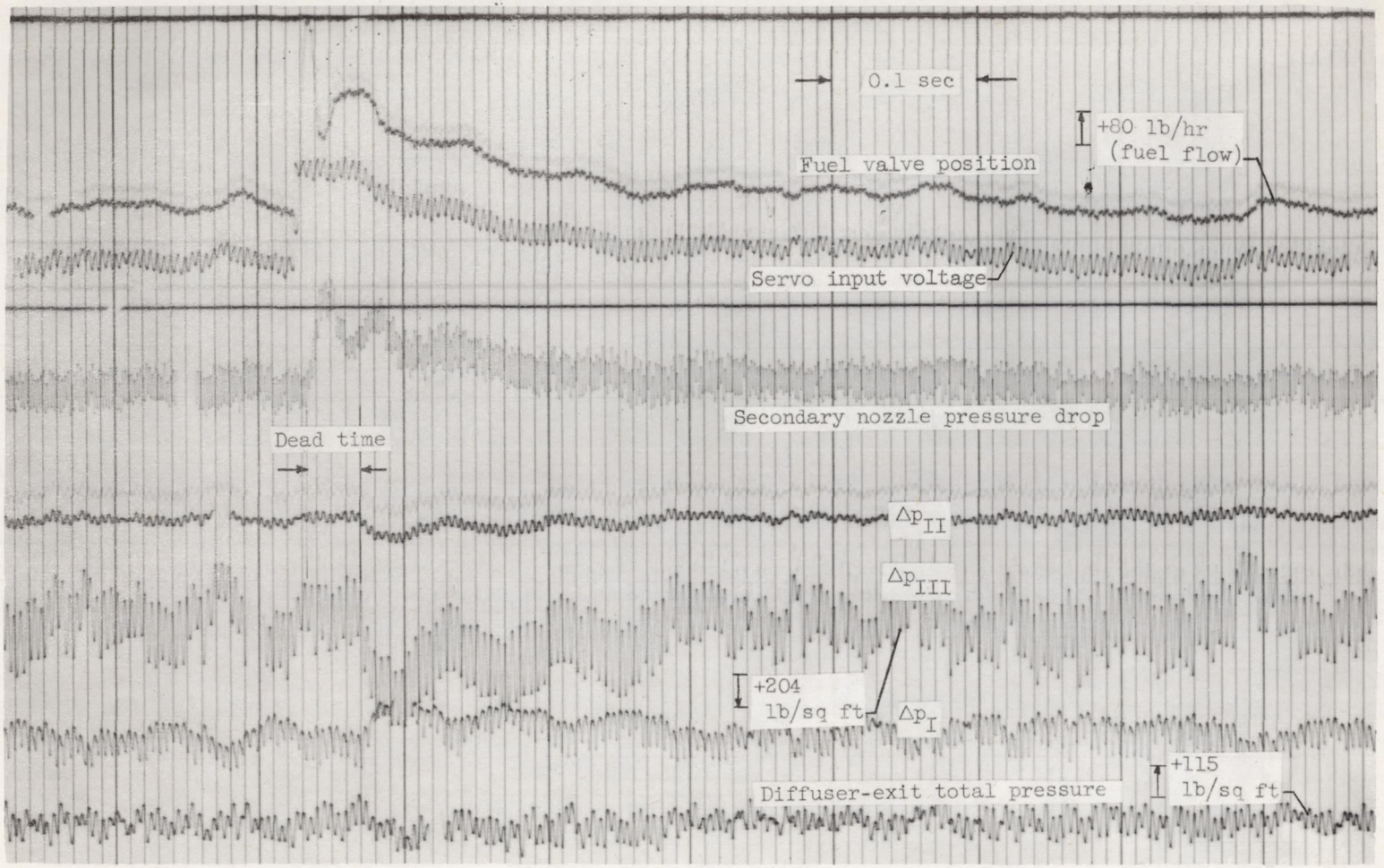

(c) Control, Δp_{III}; fuel-flow disturbance, +278 pounds per hour; loop gain, 2.40; integrator time constant, 0.02 second.

Figure 26. - Concluded. Transient response of controls to disturbance into subcritical. Free-stream Mach number, 1.98; zero angle of attack.

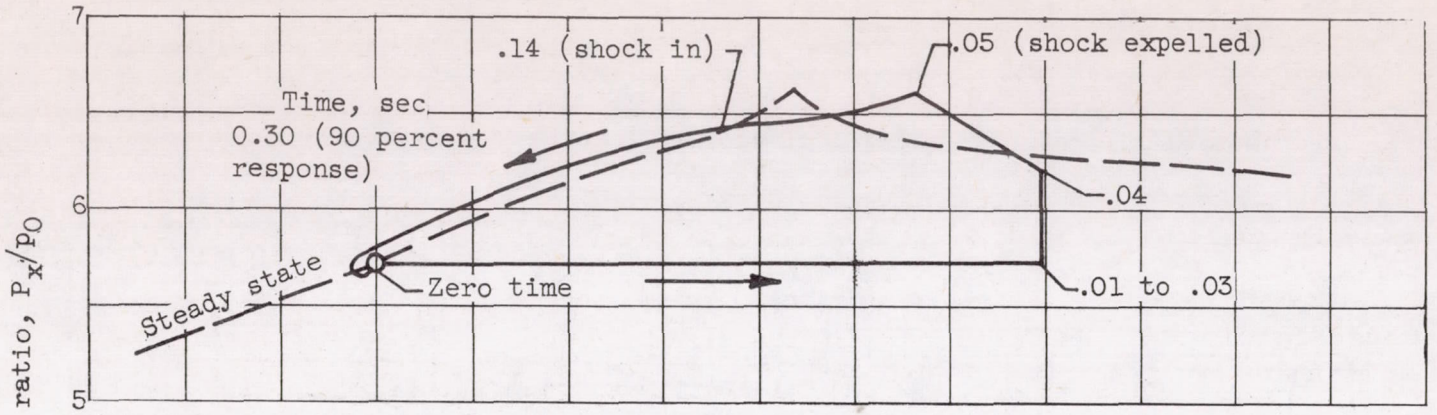

(a) Control, Δp_I; loop gain, 0.286; integrator time constant, 0.02 second.

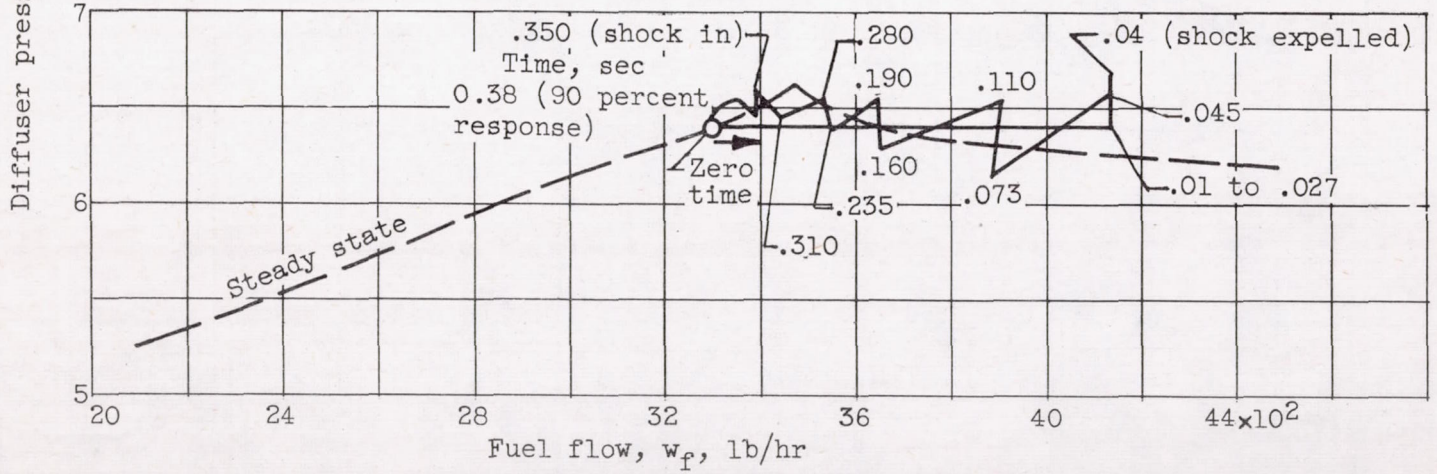

(b) Control, Δp_{II}; loop gain, 2.32; integrator time constant, 0.033 second.

Figure 27. - Transient diffuser operation of supercritical controls for disturbances causing subcritical engine operation. Free-stream Mach number, 1.98; zero angle of attack.

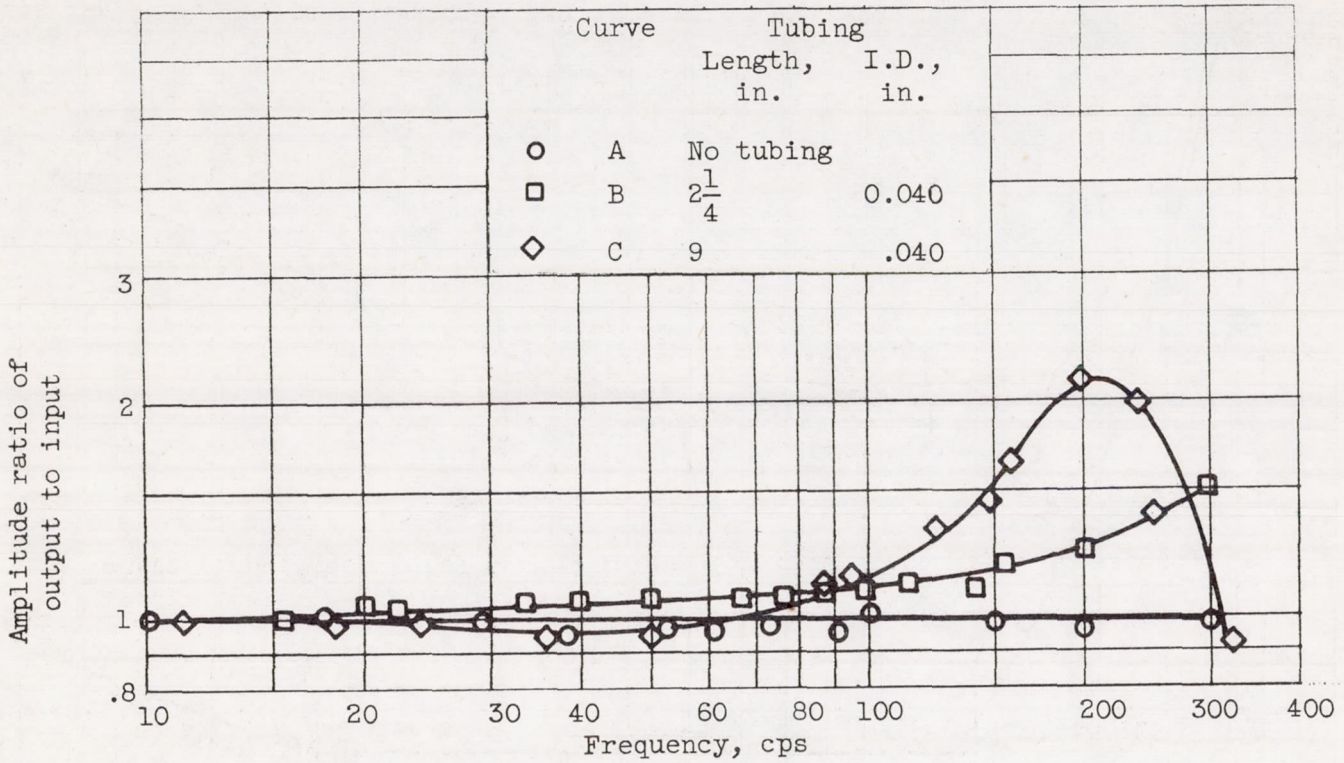

(a) Amplitude ratio.

Figure 28. - Frequency response for type I pressure transducer.

(b) Phase shift.

Figure 28. - Concluded. Frequency response for type I pressure transducer.

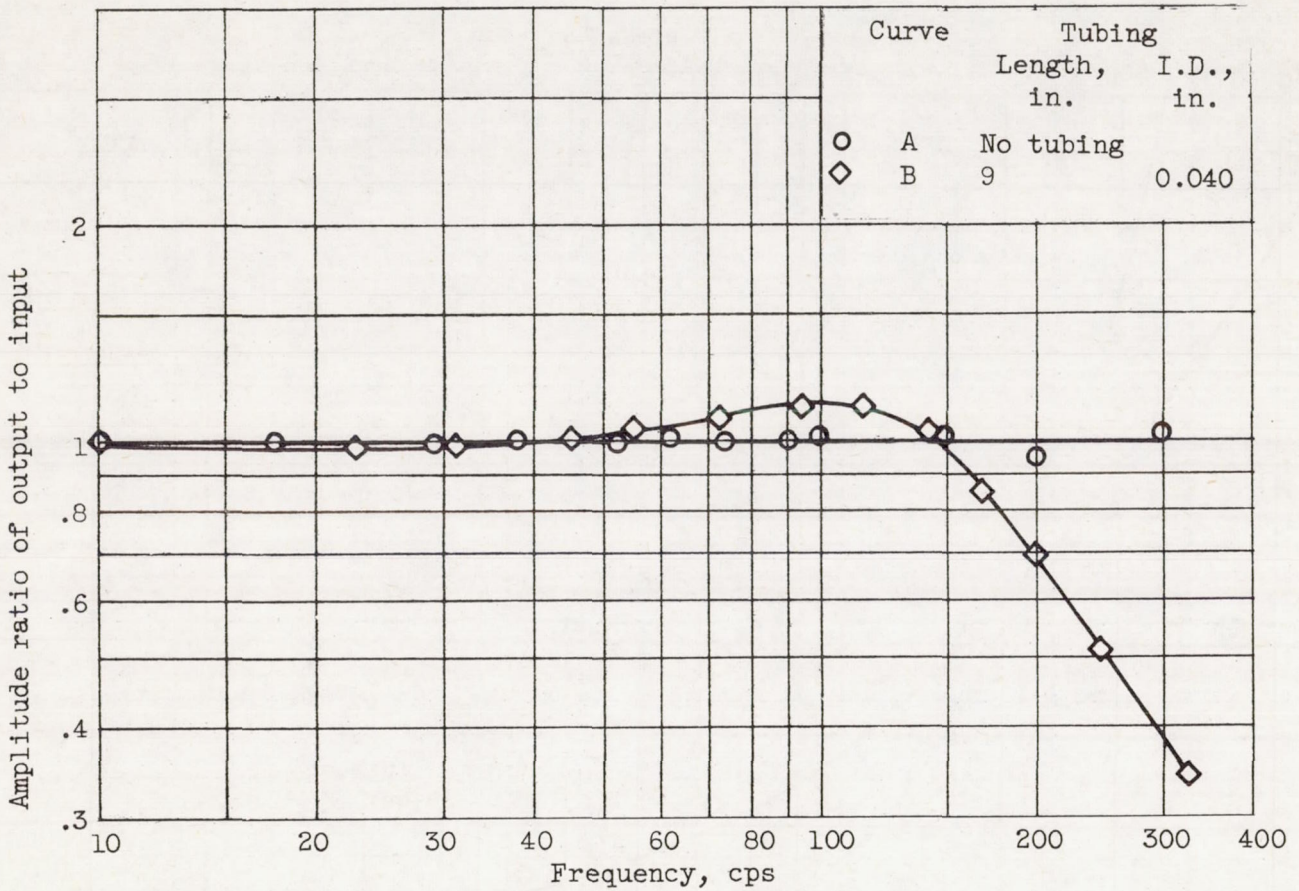

(a) Amplitude ratio.

Figure 29. - Frequency response for type II pressure transducer.

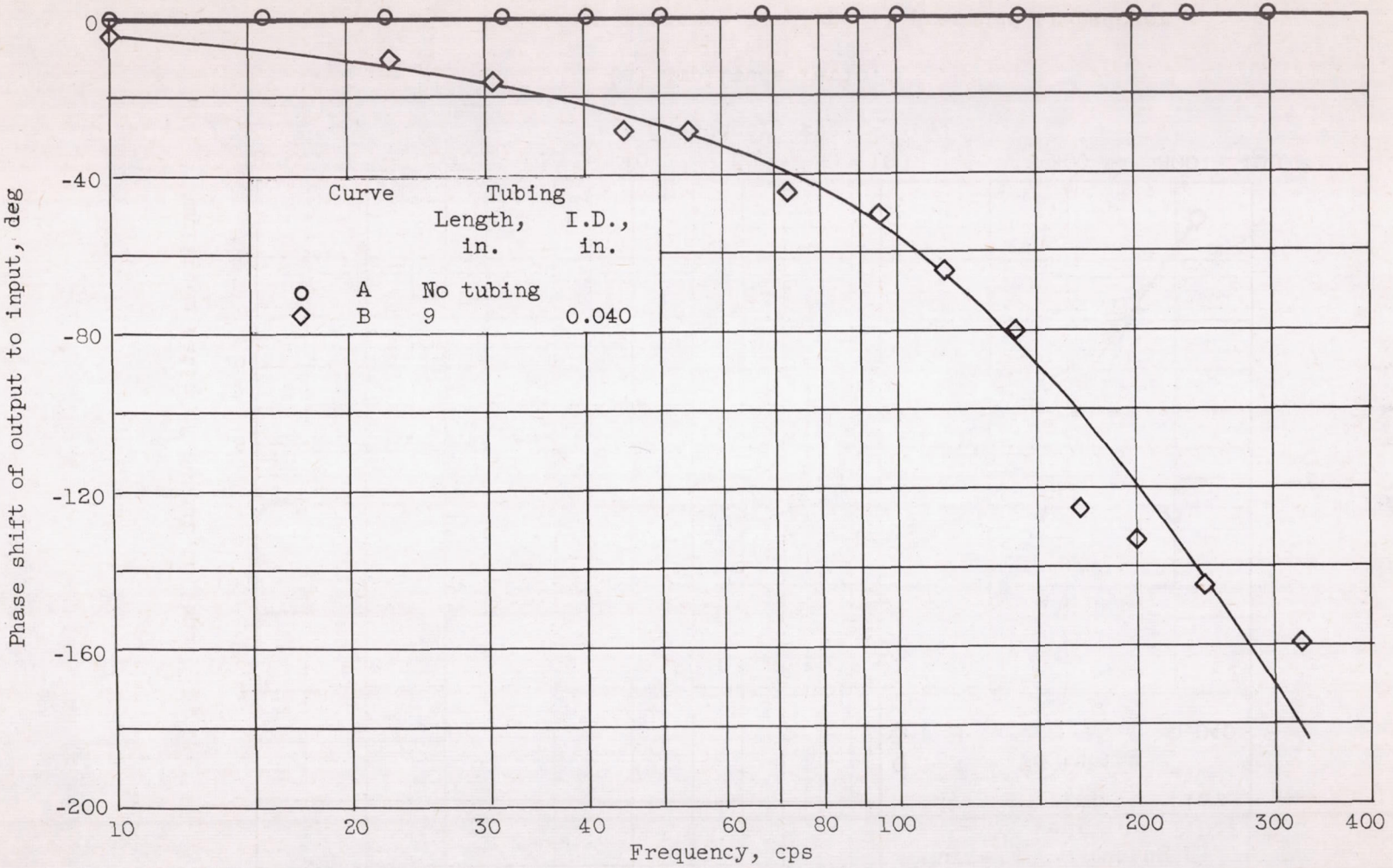

(b) Phase shift.

Figure 29. - Concluded. Frequency response for type II pressure transducer.

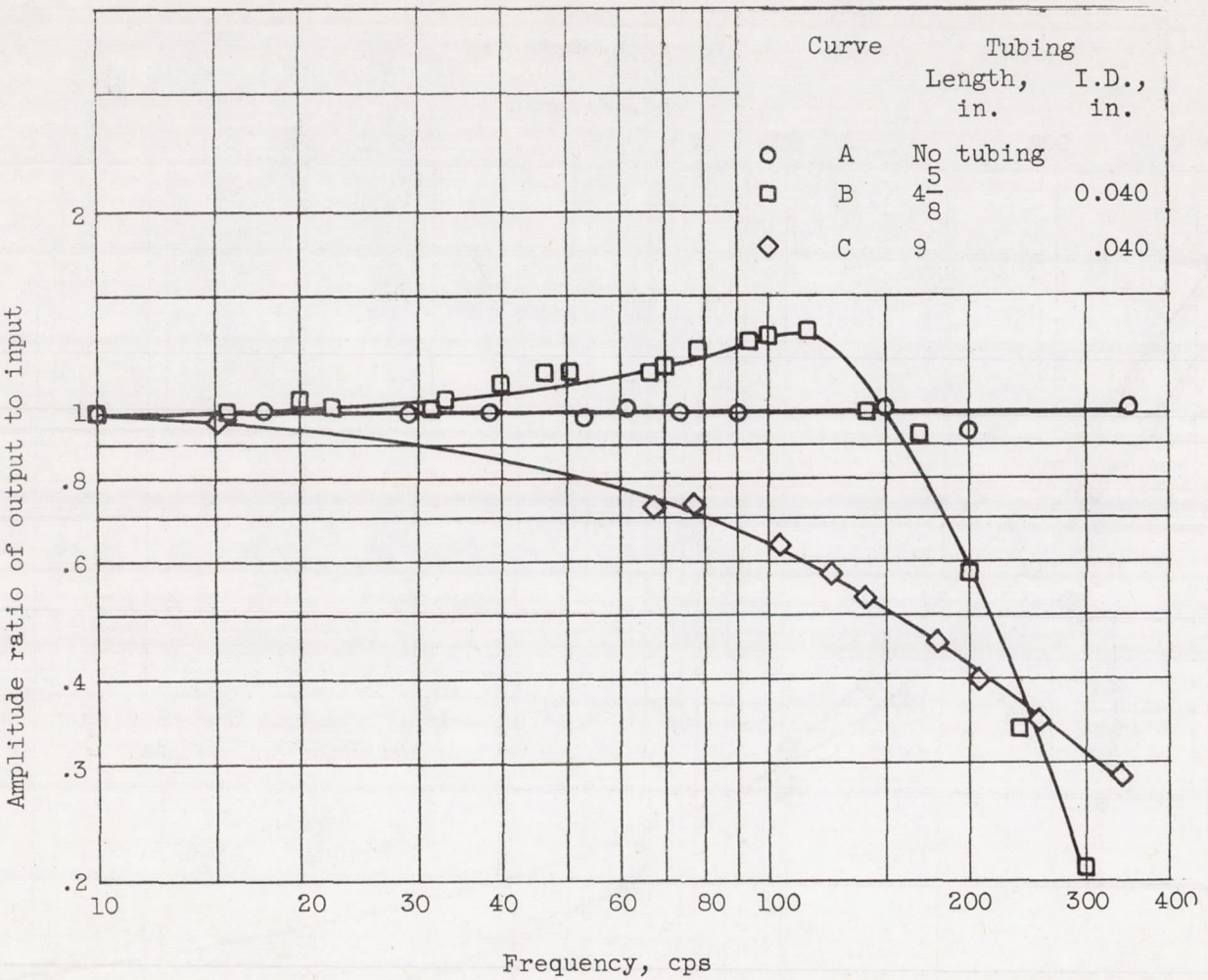

(a) Amplitude ratio.

Figure 30. - Frequency response for type III pressure transducer.

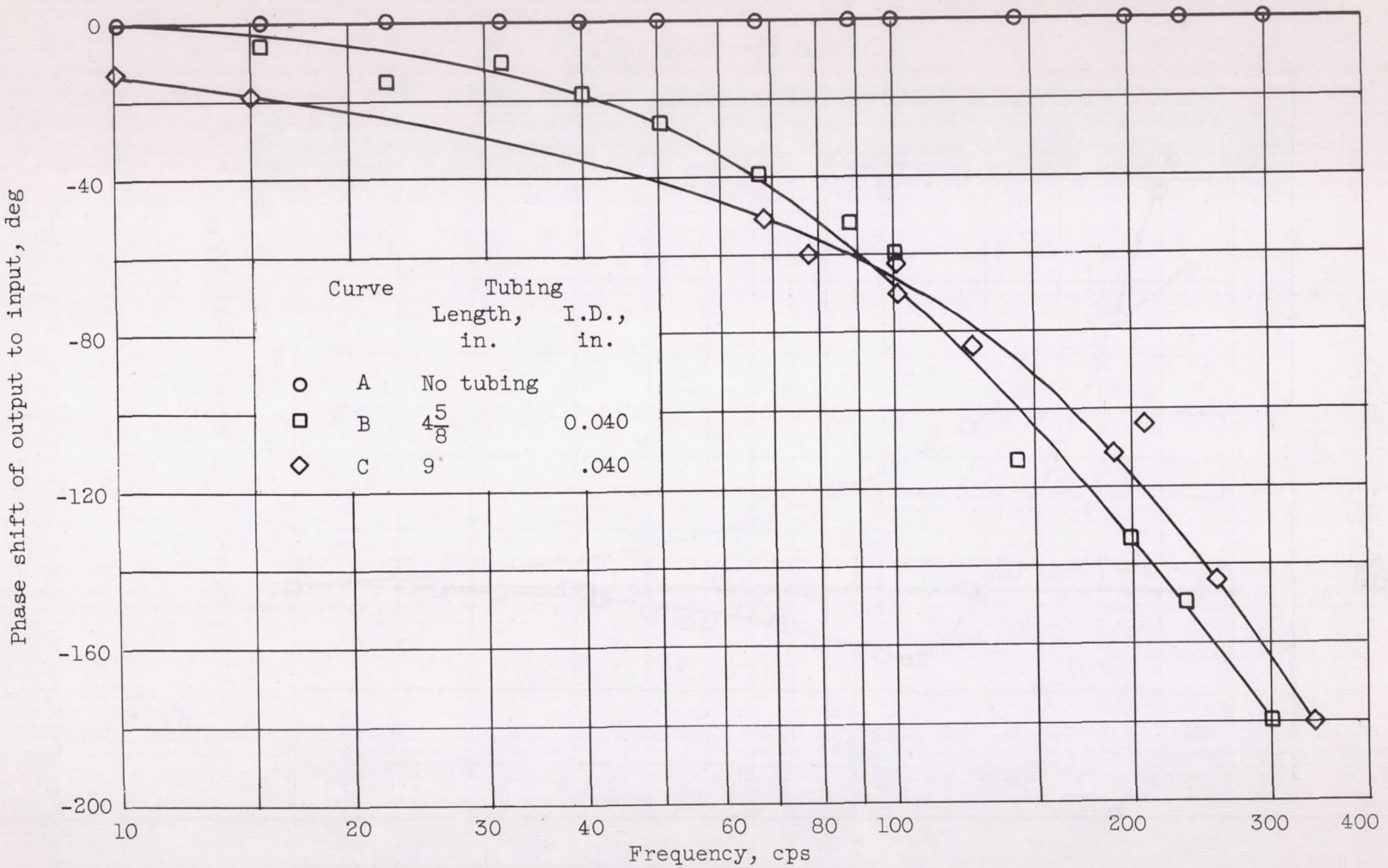

(b) Phase shift.

Figure 30. - Concluded. Frequency response for type III pressure transducer.